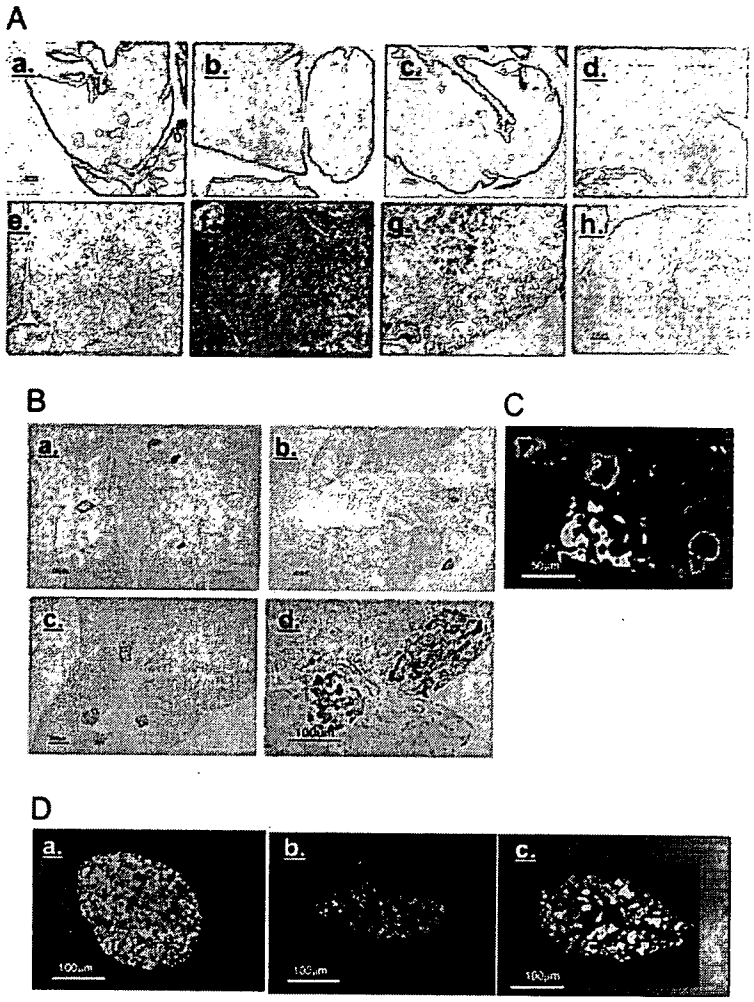

FIG. 2. Pancreatic islets of STZ-treated mice receiving subsequent BMT. A, Hematoxylin-Eosin staining of pancreases on d 35. Pancreases from normoglycemic control mouse (a and e), hyperglycemic control mouse (b and f), STZ-treated mouse simply infused with BM cells without preirradiation (c and g), and STZ-treated mouse receiving lethal irradiation and BMT (d and h). a–d, Magnification, ×40; e–h, ×100. B, Antiinsulin immunostaining of pancreases. Pancreases from normoglycemic control mouse (a), hyperglycemic control mouse (b), and STZ-treated mouse receiving BMT (c and d). a–c, Magnification, ×40; d, ×200. C, Double immunostaining of pancreas with antiinsulin and antikeratin/cytokeratin antibodies. *Green* indicates insulin-positive and *red* keratin/cytokeratin-positive cells, *i.e.* pancreatic ductal epithelium. D, Double immunostaining of pancreases with antiinsulin and antiglucagon antibodies. Pancreases from normoglycemic control mouse (a), hyperglycemic control mouse (b), and STZ-treated mouse receiving BMT (c). In C and D, to avoid overlapping staining of GFP with FITC, BM cells obtained from wild-type C57BL/6J mice, but not from GFP transgenic mice, were transplanted. Representative histological findings among six independent experiments are presented.

islets (Fig. 2A, c and g), islet number and size were both restored in STZ+BMT mice (Fig. 2A, d and h). Several islet populations were enlarged as compared with those in normoglycemic controls (Fig. 2A, a and e *vs.* d and h).

Antiinsulin staining of pancreatic specimens is shown in Fig. 2B. In hyperglycemic controls, insulin-positive cells were markedly diminished (Fig. 2B, b) as compared with normoglycemic controls (Fig. 2B, a). In contrast, in STZ+BMT mice, islet numbers were restored and sizes varied with some being enlarged (Fig. 2B, c). Notably, in the large view (Fig. 2B, d), a major population of insulin-positive cells in STZ+BMT mice is located in the vicinity of pancreatic ducts, which were stained with antikeratin/cytokeratin antibody (Fig. 2C).

Next, we performed double immunostaining using antibodies against insulin and glucagon. In immunofluorescent experiments (Figs. 2, C and D), to avoid overlapping staining of GFP with fluorescein isothiocyanate (FITC), BM cells obtained from wild-type C57BL/6J mice, but not GFP transgenic mice, were transplanted. Compared with islets of normal and STZ-treated mice (Fig. 2D, a and b), islets in STZ+BMT mice exhibited normal architecture with slightly fewer β-cells surrounded by α-cells (Fig. 2D, c).

To exclude the possibility that irradiation suppresses inflammation in response to STZ and prevents β-cell injury, STZ-treated mice were exposed to lethal irradiation (10 Gy) without subsequent BM cell infusion. Lethal irradiation alone did not lower blood glucose in STZ-treated mice. Pancreatic islets were diminished in size, as in hyperglycemic controls, 9 d after irradiation (mice died 10–14 d after lethal irradiation without BMT in our experiment; data not shown). Next, to examine prolonged effects of irradiation, mice were sublethally irradiated (5 Gy). Sublethal irradiation alone likewise did not significantly improve hyperglycemia in STZ-treated mice (data not shown), suggesting that irradiation does not exert protective effects against STZ-induced β-cell injury.

To further examine whether these islets in STZ+BMT mice were regenerated or only protected from STZ injury, BrdU staining was performed. In islets of normoglycemic (Fig. 3A) and hyperglycemic (Fig. 3B) controls, there were very few BrdU-positive cells. In contrast, islets of STZ+BMT mice (10 d after BMT) contained substantial numbers of BrdU-positive cells in and around islets, and some were detected among the pancreatic ductal cells (Fig. 3C). In other sections as well, islets containing BrdU-positive cells were mostly located near ducts and blood vessels. Most BrdU-positive cells in islets were insulin positive, whereas those outside the islets, mostly in the ductal structure, did not express insulin.

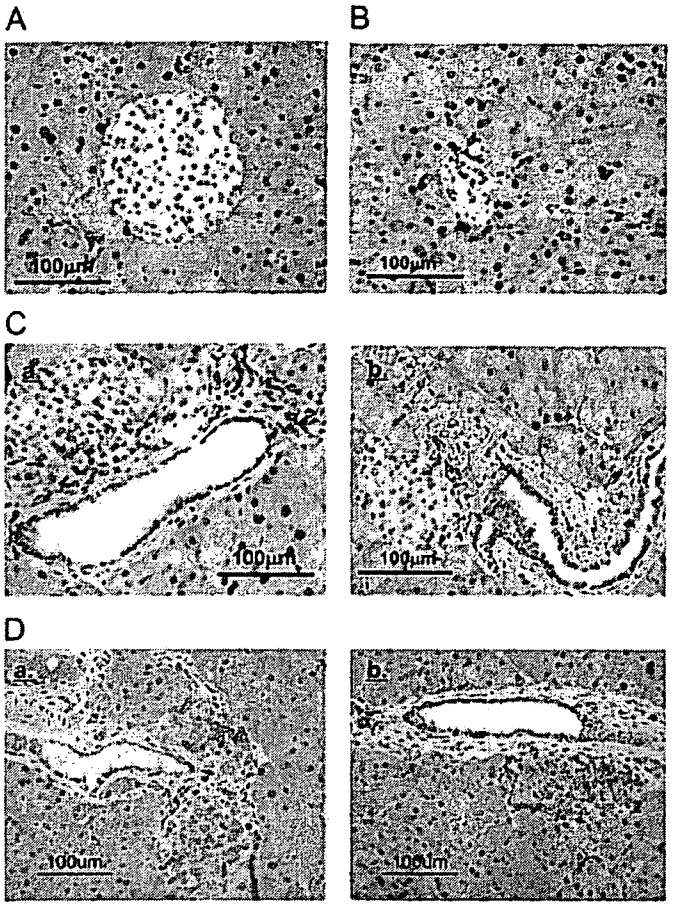

FIG. 3. BrdU-positive proliferating cells in pancreases of STZ-treated mice receiving subsequent BMT. A–C, Pancreases from normoglycemic control mouse (A), hyperglycemic control mouse (B), and STZ-treated mice receiving BMT (C) (10 d after BMT). *Brown cells* are BrdU positive. D, Double immunostaining of pancreases from STZ-treated mice receiving BMT (10 d after BMT) with antiinsulin and anti-BrdU. *Brown* and *red cells* are BrdU and insulin positive, respectively.

(Fig. 3D). Given reports that pancreatic stem/progenitor cells exist among ductal cells (24–26), BMT after STZ treatment might stimulate the generation of new islets from ductal progenitor cells as well as proliferation of β-cells in this model.

We also quantitatively examined the time courses of islet numbers, cell number per islet and percentage of BrdU-positive cells among islet cells after BMT (Table 1). Although decreased by STZ, islet number was significantly increased 10 and 15 d after BMT. The peak islet number was greater than in normoglycemic control mice by 47%. The islet number and percentage of BrdU-positive cells among islet cells were also increased through 10 d after BMT and then fell to normoglycemic control levels. These findings clearly indicate that BMT induces β-cell regeneration, resulting in pancreatic islet restoration in this model.

Although no BM-derived insulin-positive cells were detected, the regenerated islets were surrounded by BM-derived CD45-positive cells

To investigate whether BM-derived cells transdifferentiated into insulin-producing cells in our model, pancreases from STZ+BMT mice on d 35 were immunostained with antiinsulin antibody, followed by an intensive search for both insulin- and GFP-positive cells using confocal fluorescence microscopy. However, no double-positive cells were detected (Fig. 4A), suggesting that regenerated β-cells in STZ+BMT mice are derived from recipient cells. In contrast, intriguingly, GFP-positive, *i.e.* BM-derived, cells were located around islets (Fig. 4A). In STZ+BM-infused mice, no GFP-positive cells were detected around islets (data not shown). Immunostaining with anti-GFP antibody confirmed that GFP-positive cells exist around islets of STZ+BMT mice (Fig. 4B, *black arrows* indicate islets). To identify the lineage of BM-derived cells around islets, we used several antibodies to immunostain lineage markers. GFP-positive cells around islets were CD45-positive (Fig. 4C, *white arrows* indicate islets), although these cells were not positively stained with F4/80, CD68 (macrophage lineage), CD3/CD5 (T cell lineage), or CD20 (B cell lineage) (data not shown), suggesting immature hematopoietic cells. We additionally examined whether these BM-derived cells are positive for an endothelial cell marker, CD31 (PECAM-1). Although a few GFP-positive cells were positive for CD 31 (Fig. 4D, *red arrow*), most BM-derived cells in or around islets were not positively stained with this endothelial marker. Taken together, these observations suggest that donor immature hematopoietic cells, which may be expanded and mobilized to peripheral blood after BMT, initiate β-cell regeneration.

Mobilization of BM-derived cells is necessary for the glucose-lowering effect of BMT after STZ administration

To determine whether BM-derived cell mobilization is pivotal in this process, we investigated the effects of BMT on

TABLE 1. Islet numbers and BrdU-positive cells per pancreatic islet cells of STZ-treated mice receiving subsequent BMT

	Days after BMT	Nos. of islets	Nos. of BrdU-positive cells	Nos. of cells in islets	Percentage of BrdU-positive cells among islet cells
STZ(−) control		94.0 ± 17.3	33.3 ± 4.5	7174 ± 1487	0.51 ± 0.08
	0	62.0 ± 11.9	20.6 ± 5.6	4658 ± 1019	0.47 ± 0.11
	3	48.3 ± 2.0	40.7 ± 16.2	2974 ± 278	1.41 ± 0.51
STZ+BMT (days after BMT)	7	102.7 ± 11.6	194.3 ± 33.4[a]	6159 ± 528	3.10 ± 0.31[a]
	10	138.0 ± 22.9[a]	253.0 ± 107.8[a]	7989 ± 756[a]	3.40 ± 1.63
	15	113.7 ± 6.9[a]	64.7 ± 16.3	5223 ± 539	1.34 ± 0.40
	25	82.0 ± 6.4	37.5 ± 0.4	3953 ± 157	0.95 ± 0.03

To calculate numbers of islets and cells per islet and the percentage of BrdU-positive cells among islet cells, we microscopically examined the whole pancreas in 30-μm sections and counted the numbers of islets, islet cells, and BrdU-positive nuclei in islets.

[a] $P < 0.05$ *vs.* d 0 in STZ+BMT group.

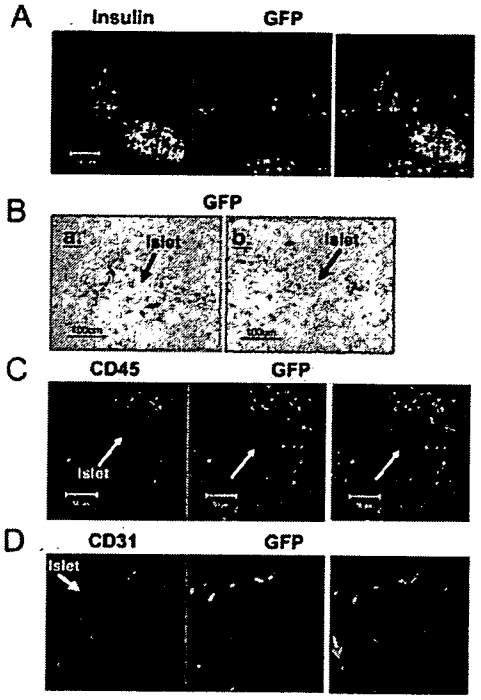

FIG. 4. BM-derived cells in pancreases of STZ-treated mice receiving subsequent BMT. A, BM-derived cells and insulin-positive cells in pancreas of STZ-treated mouse receiving BMT from GFP transgenic mice. Pancreases of STZ-treated mouse receiving subsequent BMT from GFP transgenic mice (35 d after the first STZ). *Left panel*, Insulin-positive cells; *middle panel*, GFP-positive, *i.e.* BM-derived cells; *right panel*, merged image of the *left* and *middle panels*. B, BM-derived cells in pancreases of STZ-treated mice receiving BMT from GFP transgenic mice. *Brown cells* are GFP positive, *i.e.* BM-derived cells, and *arrows* indicate islets. C, CD45-positive and BM-derived cells in pancreas of STZ-treated mice receiving BMT from GFP transgenic mice. *Left panel*, Immunostaining with anti-CD45 antibody. *Red* indicates CD45-positive cells. *Middle panel*, *Green* indicates GFP-positive cells. *Right panel*, Merged image of the *left* and *middle panels*. *Yellow* indicates GFP and CD45 double-positive cells. *Arrows* indicate islets. D, CD31 (PECAM-1)-positive and BM-derived cells in pancreases of STZ-treated mice receiving BMT from GFP transgenic mice. *Left panel*, Immunostaining with anti-CD31 antibody. *Red* indicates CD31-positive cells. *Middle panel*, *Green* indicates GFP-positive cells. *Right panel*, Merged image of *left* and *middle panels*.

β-cell regeneration using eNOS-deficient ($Nos3^{-/-}$) mice as a model for impaired BM-derived cell mobilization. In $Nos3^{-/-}$ mice, mobilizations of hematopoietic stem cells and endothelial progenitor cells from BM were reportedly impaired after myelosuppression. Deficiency in eNOS reportedly reduces hematopoietic recovery in response to 5-fluorouracil treatment due to impaired progenitor cell mobilization (20). Therefore, we performed similar experiments using $Nos3^{-/-}$ mice. First, we compared two BMT groups, *i.e.* $Nos3^{+/+}$ donors to $Nos3^{+/+}$ recipients ($Nos3^{+/+}$ *to* $Nos3^{+/+}$ mice) and $Nos3^{-/-}$ donors to $Nos3^{-/-}$ recipients ($Nos3^{-/-}$ to $Nos3^{-/-}$ mice).

Peripheral white blood cells (WBCs) were counted after lethal irradiation and subsequent BM infusion (Fig. 5A). Myelosuppression after irradiation was profound and recovery of peripheral WBC counts was markedly delayed in $Nos3^{-/-}$ to $Nos3^{-/-}$ mice *vs.* $Nos3^{+/+}$ to $Nos3^{+/+}$ mice. Thus, eNOS deficiency impairs hematopoietic reconstitution after not only 5-fluorouracil treatment but also BMT. We measured the blood glucose levels after STZ administration followed by BMT (Fig. 5B). In $Nos3^{+/+}$ to $Nos3^{+/+}$ mice, STZ-induced hyperglycemia was improved to nearly normoglycemic control levels 40 d after the first STZ administration, consistent with the findings shown in Fig. 1C. In contrast, in $Nos3^{-/-}$ to $Nos3^{-/-}$ mice, BMT did not improve STZ-induced hyperglycemia (Fig. 5B). Thus, eNOS function is essential for improving hyperglycemia after BMT.

In $Nos3^{-/-}$ to $Nos3^{-/-}$ mice, not only mobilization of BMT-derived progenitor cells but also pancreatic endothelial function may be impaired due to systemic eNOS deficiency. Therefore, we performed an additional BMT, *i.e.* $Nos3^{-/-}$ donors to $Nos3^{+/+}$ recipients ($Nos3^{-/-}$ to $Nos3^{+/+}$ mice), whose eNOS is intact in pancreatic blood vessels. In $Nos3^{-/-}$ to $Nos3^{+/+}$ mice, myelosuppression was profound and subsequent recovery of the WBC count was delayed, compared with $Nos3^{+/+}$ to $Nos3^{+/+}$ mice, but this delay in recovery was significantly less severe than that seen in $Nos3^{-/-}$ recipients (Fig. 5A). In $Nos3^{-/-}$ to $Nos3^{+/+}$ mice, blood glucose levels also reached midrange values; the glucose-lowering effects of BMT did occur but were significantly blunted (Fig. 5B). These findings indicate that the lack of hyperglycemia improvement in $Nos3^{-/-}$ to $Nos3^{-/-}$ mice is not attributable solely to the impaired pancreatic endothelial function of recipients. The glucose-lowering effect of BMT inversely correlates with the severity of myelosuppression and delayed recovery, which apparently reflects impaired mobilization of BM cells to peripheral blood.

BMT-induced β cell regeneration was impaired in STZ-treated $Nos3^{-/-}$ mice

To quantify BMT-induced β-cell regeneration in $Nos3^{+/+}$ to $Nos3^{+/+}$ and $Nos3^{-/-}$ to $Nos3^{-/-}$ mice, pancreatic insulin contents 40 d after STZ (30 d after BMT) were measured (Fig. 5C). Compared with $Nos3^{+/+}$ controls without STZ treatment, STZ-treated $Nos3^{+/+}$ mice had markedly lower pancreatic insulin contents. In $Nos3^{+/+}$ to $Nos3^{+/+}$ mice, BMT partially restored pancreatic insulin contents, consistent with our findings that plasma insulin levels were partially restored by BMT (Fig. 1D). In contrast, in $Nos3^{-/-}$ to $Nos3^{-/-}$ mice, BMT effects on pancreatic insulin contents were very limited; pancreatic insulin contents were significantly lower in $Nos3^{-/-}$ to $Nos3^{-/-}$ mice than in $Nos3^{+/+}$ to $Nos3^{+/+}$ mice (Fig. 5C).

Next, changes in islet numbers and percentage of BrdU-positive cells among islet cells in response to BMT were compared between $Nos3^{+/+}$ to $Nos3^{+/+}$ mice and $Nos3^{-/-}$ to $Nos3^{-/-}$ mice. Whereas islet numbers were increased in STZ-treated $Nos3^{+/+}$ to $Nos3^{+/+}$ mice during the period 7–15 d after BMT, islet numbers were significantly less in STZ-treated $Nos3^{-/-}$ to $Nos3^{-/-}$ mice (Fig. 5D). In addition, whereas percentages of BrdU-positive cells among islet cells were markedly increased in STZ-treated $Nos3^{+/+}$ to $Nos3^{+/+}$ mice 7–10 d after BMT, there were significantly fewer such cells in STZ-treated $Nos3^{-/-}$ to $Nos3^{-/-}$ mice (Fig. 5E). These results suggest that impaired BM-derived cell mobilization

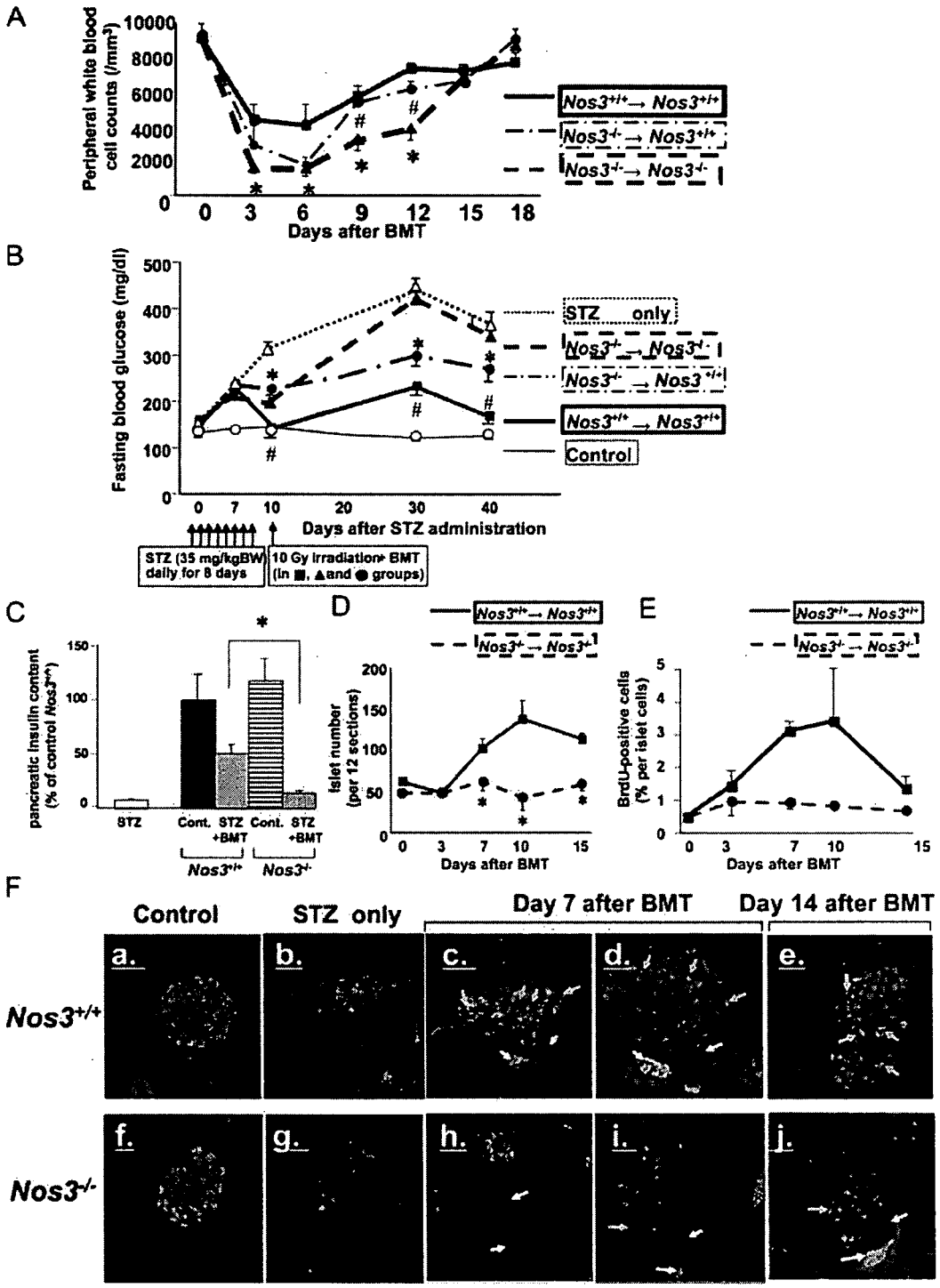

FIG. 5. BMT experiments using *Nos3*$^{+/+}$ and *Nos3*$^{-/-}$ mice. A, Time courses of peripheral WBC counts in *Nos3*$^{+/+}$ and *Nos3*$^{-/-}$ mice receiving BMT. ■, STZ-treated *Nos3*$^{+/+}$ mice receiving BMT from *Nos3*$^{+/+}$ mice; ▲, STZ-treated *Nos3*$^{-/-}$ mice receiving BMT from *Nos3*$^{-/-}$ mice; ●, STZ-treated *Nos3*$^{+/+}$ mice receiving BMT from *Nos3*$^{-/-}$ mice. *, $P < 0.05$ for ▲, compared with ■ group; #, $P < 0.05$ for ●, compared with ▲ group, respectively (n = 5–6 in each group). B, Fasting blood glucose levels of *Nos3*$^{-/+}$ and *Nos3*$^{-/-}$ receiving BMT. ○, Normoglycemic control *Nos3*$^{+/+}$ mice with neither STZ nor BMT; △, STZ-treated *Nos3*$^{+/+}$ mice without BMT (hyperglycemic control); ■, STZ-treated *Nos3*$^{+/+}$ mice receiving BMT from *Nos3*$^{+/-}$ mice; ▲, STZ-treated *Nos3*$^{-/-}$ mice receiving BMT from *Nos3*$^{-/-}$ mice; ●, STZ-treated *Nos3*$^{+/+}$ mice receiving BMT from *Nos3*$^{-/-}$ mice. *, $P < 0.05$ for ●, compared with △ group; # $P < 0.05$ for ■, compared with ● group, respectively (n = 5–6 in each group). C, Pancreatic insulin contents. STZ, STZ-treated *Nos3*$^{+/+}$ mice without BMT; Cont, *Nos3*$^{+/+}$ or *Nos3*$^{-/-}$ mice with neither STZ nor BMT; STZ+BMT, STZ-treated *Nos3*$^{+/+}$ mice receiving BMT from *Nos3*$^{+/+}$ mice and STZ-treated *Nos3*$^{-/-}$ mice receiving BMT from *Nos3*$^{-/-}$ mice. *, $P < 0.05$ between STZ-treated *Nos3*$^{+/+}$ mice receiving BMT from *Nos3*$^{+/+}$ mice and STZ-treated *Nos3*$^{-/-}$ mice receiving BMT from *Nos3*$^{-/-}$mice. D, Time courses of islet numbers after BMT. E, Time courses of BrdU-positive cell percentage per islet cells after BMT. In D and

in $Nos3^{-/-}$ mice suppresses BMT-induced β-cell regeneration after acute injury.

BM-derived CD45-positve cells around islets are important for β-cell regeneration-induced by BMT

To examine whether impaired mobilization of BM-derived cells in $Nos3^{-/-}$ mice affects hematopoietic cell assembly around islets and β-cell regeneration, we compared pancreases from $Nos3^{+/+}$ to $Nos3^{+/+}$ and $Nos3^{-/-}$ to $Nos3^{-/-}$ mice using antiinsulin and CD45 antibodies (Fig. 5F). In $Nos3^{+/+}$ to $Nos3^{+/+}$ mice, substantial numbers of CD45-positive cells were detected in and around the regenerated islets (*red arrows* in Fig. 5F, c–e). No such cells were detected around islets in $Nos3^{+/+}$ or $Nos3^{-/-}$ mice treated with STZ alone (Fig. 5F, b and g), suggesting that STZ-induced inflammation alone is not responsible for recruiting these cells. In pancreases from $Nos3^{+/+}$ to $Nos3^{+/+}$ mice, regenerated islets were located near pancreatic ducts and blood vessels (*white arrows* in Fig. 5F, c–e). In contrast, β-cell regeneration was markedly impaired in $Nos3^{-/-}$ to $Nos3^{-/-}$ mice (Fig. 5F, h–j), and far fewer CD45-positive cells were present in and around islets in $Nos3^{-/-}$ to $Nos3^{-/-}$ than in $Nos3^{+/+}$ to $Nos3^{+/+}$ mice. These results support the notion that BMT-induced BM-derived cell mobilization is critical for regeneration of recipient β-cells from stem/progenitor cells in pancreatic ducts.

Discussion

Recently considerable research attention has focused on pancreatic β-cell regeneration. In particular, several previous studies examined the role of BM-derived cells in β-cell regeneration using BMT (10–18), but no definitive conclusions have yet been reached. In this study, we clearly demonstrate that BMT can regenerate recipient β-cells under certain conditions. Our data supported those of a previous report (14) showing BMT to improve hyperglycemia in STZ-induced diabetic mice via regeneration of recipient pancreatic β-cells. Herein we attempted to elucidate the mechanisms whereby BMT induces β-cell regeneration.

First, we demonstrated that BMT, but not simple BM cell infusion without preirradiation, promotes β-cell regeneration after STZ-induced injury. What are the differences between these procedures? BMT involves lethal irradiation and subsequent BM cell infusion. We confirmed, using FACS analysis, that recipient BM is essentially replaced with that of donor mice after BMT. In contrast, mice receiving BM cell infusion alone without preirradiation showed no BM replacement with donor-derived cells. Myelosuppression and subsequent expansion of donor BM cells take place in BMT. During this process, donor BM cells home to the BM microenvironment and progenitor cells mobilize and expand in the peripheral blood (27). In contrast, simple BM cell infusion does not induce homing or expansion of donor BM cells. Therefore, expansion of immature BM cells, which are rarely detected in peripheral blood in normal circumstances, is likely to be important for β-cell regeneration after BMT. We ruled out the possibility that irradiation suppresses inflammation in response to STZ administration and prevents β-cell injury. STZ-treated mice were exposed to lethal (10 Gy) and sublethal (5 Gy) irradiation without subsequent BM cell infusion. Irradiation alone had no effect on hyperglycemia or β-cell number in STZ-treated mice. Furthermore, in STZ+BMT mice on d 2 after BMT, islet numbers and cell numbers per islet were both significantly decreased by STZ but were restored by d 10. Thus, it is unlikely that irradiation itself protects β-cells.

Next, we found that a major population of post-BMT islets were located near pancreatic ducts and blood vessels. This observation raises possibilities regarding the origins of post-BMT islets. In general, multipotent adult stem cells are located in somatic tissues, which maintain and regenerate impaired tissues (28, 29). However, there is considerable controversy regarding the existence and location of pancreatic tissue stem cells (30, 31). Previous studies have shown pancreatic stem/progenitor cells in ductal epithelium (24–26). However, recent reports suggest that β-cells arise only from self-duplication of preexisting β-cells, *i.e.* β-cells cannot be derived from non-β-cell progenitors (32, 33). In this study, post-BMT islets were located near pancreatic ducts. In addition, BrdU-positive cells were detected in the vicinity of pancreatic ducts in STZ+BMT mice. After islet numbers had been decreased by STZ, a rise above normoglycemic control levels was seen, indicating new islet formation. In addition, BM-derived cells accumulated in and around post BMT-islets. Thus, BM-derived cells are likely to stimulate proliferation and differentiation of pancreatic stem/progenitor cells in ductal epithelium, resulting in new islet formation. Given the observation that BrdU-positive cells in islets expressed insulin, these cells must still have been proliferative after differentiation into pancreatic β-cells. However, further studies, focusing on the origin of newly generated islets, are needed to support this speculation. Whereas BM-derived cells that accumulated around the islets in STZ+BMT mice were CD45 positive, immunohistochemical studies revealed that these cells do not express mature T or B lymphocyte or macrophage markers. Taken together with the finding that simple BM infusion without preirradiation induced neither β-cell regeneration nor accumulation of BM-derived cells (data not shown), we speculate that these immature BM-derived cells send signals triggering proliferation and differentiation of stem/progenitor cells into β-cells. Our next goal is identification of these signals.

To examine the causal relationship between BM-derived cell mobilization and BMT-induced β-cell regeneration, we performed similar experiments using a model of impaired

E, the *thick line* indicates STZ-treated $Nos3^{+/+}$ mice receiving BMT from $Nos3^{+/+}$ mice, and the *dotted line* STZ-treated $Nos3^{-/-}$ mice receiving BMT from $Nos3^{-/-}$ mice. *, $P < 0.05$ between STZ-treated $Nos3^{+/+}$ mice receiving BMT from $Nos3^{+/+}$ mice and STZ-treated $Nos3^{-/-}$ mice receiving BMT from $Nos3^{-/-}$mice at the same time points. F, Immunostaining of pancreases with antiinsulin and anti-CD45 antibodies. Pancreases from normoglycemic control mice ($Nos3^{+/+}$ mouse in a and $Nos3^{-/-}$ mouse in f), hyperglycemic control mice ($Nos3^{+/+}$ mouse in b and $Nos3^{-/-}$ mouse in g), STZ-treated $Nos3^{+/+}$ mice receiving BMT from $Nos3^{+/+}$ mice (7 d after BMT in c and d, 14 d after BMT in e), and STZ-treated $Nos3^{-/-}$ mice receiving BMT from $Nos3^{-/-}$ mice (7 d after BMT in h and i, 14 d after BMT in j). *Green* indicates insulin-positive, *red* CD45-positive cells. *Red arrows* indicate CD45-positive cells in and around islets and *white arrows* pancreatic ducts and blood vessels.

BM-derived cell mobilization. Mechanisms underlying mobilization of hematopoietic and endothelial progenitor cells from BM after myelosuppression have been studied in detail (34). After myelosuppression, secreted cytokines/chemokines, such as granulocyte-colony stimulating factor, stromal cell-derived factor, and vascular endothelial growth factor, activate matrix metalloproteinase (MMP)-9 in the BM microenvironment. Activated MMP-9 processes membrane-bound kit-ligand, releases it as soluble kit-ligand (sKitL), followed by binding of sKitL to c-*kit* on the stem cell surface and stimulation of its mobilization from the BM. Because nitric oxide from BM is necessary for MMP-9 activation, sKitL production and the resultant mobilization of BM-derived cells are impaired in *Nos3*$^{-/-}$ mice (20). Therefore, using *Nos3*$^{-/-}$ mice, we examined the effects of BMT on blood glucose levels and glucose β-cell regeneration. We first confirmed that recovery of the WBC count after BMT was significantly delayed in *Nos3*$^{-/-}$ to *Nos3*$^{-/-}$ mice, compared with *Nos3*$^{+/+}$ to *Nos3*$^{+/+}$ mice. Judging from the doubling time of hematopoietic cells, a 1-wk delay in WBC recovery indicates marked impairment of BM cell mobilization by approximately 2 orders of magnitude. In *Nos3*$^{-/-}$ to *Nos3*$^{-/-}$ mice, BMT had virtually no effects on blood glucose levels, pancreatic insulin contents, islet numbers, or percentage of BrdU-positive cells among islet cells. In addition, far fewer CD45-positive cells were detected in and around islets. These results support the notion that BMT-induced BM-derived cell mobilization plays a pivotal role in β-cell regeneration from ductal progenitor cells.

Neovascularization in ischemic regions is also impaired in *Nos3*$^{-/-}$ mice because of decreased mobilization of BM-derived endothelial progenitor cells (20). The microvasculature is well developed in pancreatic islets (35). Endothelial signals are reportedly important for islet development (36), insulin gene expression, and β-cell proliferation (37). In the present study, a small population of BM-derived cells around regenerated islets was positively stained with CD31, although these cells were largely CD31 negative. This observation is consistent with the results of previous report (14). Therefore, in addition to hematopoietic progenitor cells, endothelial progenitor cells mobilized from BM may contribute to β-cell regeneration after BMT by promoting islet microvasculature formation. In addition, BM-derived endothelial progenitor cells have been shown to contribute to neovascularization in impaired tissues, including myocardial (38) and hind limb ischemia (39). Recruitment of these cells reportedly occurs in response to acute injury of β-cells (19). Taken together with the finding that, when BMT was performed 30 d after STZ treatment, hyperglycemia-improving effects were far smaller, acute STZ injury might trigger migration of immature BM-derived cells to the injured pancreas.

We do not rule out the importance of eNOS in pancreatic blood vessels for BMT-induced β-cell regeneration. However, in *Nos3*$^{-/-}$ to *Nos3*$^{+/+}$ mice, which have decreased BM eNOS (because of BM replacement with eNOS-deficient cells) with intact pancreatic eNOS, the blood glucose-lowering effects of BMT were significantly blunted, compared with *Nos3*$^{+/+}$ to *Nos3*$^{+/+}$ mice. Thus, glucose-lowering effects correlated inversely with the severity of myelosuppression and delayed recovery of the peripheral WBC count, suggesting the importance of BM-derived cell mobilization, rather than eNOS activity in pancreatic blood vessels, in BMT-induced β-cell regeneration.

In summary, BMT promotes β-cell regeneration after STZ-induced injury. A series of BMT experiments using *Nos3*$^{-/-}$ mice demonstrated BM-derived cell mobilization to be essential for BMT-induced β-cell regeneration. Acute injury with STZ treatment may trigger recruitment of immature BM-derived cells to the injured pancreas. Recruited BM-derived cells may then stimulate stem/progenitor cells located in the recipient pancreas, resulting in islet regeneration. To our knowledge, this is the first report showing mobilization of BM-derived cells to be involved in β-cell regeneration in diabetic animals. From the viewpoint of clinical application, it is important to study the effects of myelosuppression-inducing reagents, such as antitumor drugs, on pancreatic islet regeneration.

Acknowledgments

The authors thank Dr. M. Okabe for providing GFP transgenic mice and are indebted to M. Hoshi, I. Sato, K. Kawamura, and J. Fushimi, who assisted with various aspects of this study.

Received October 5, 2006. Accepted January 18, 2007.

Address all correspondence and requests for reprints to: Hideki Katagiri, M.D., Ph.D., Division of Advanced Therapeutics for Metabolic Diseases, Center for Translational and Advanced Animal Research, Tohoku University Graduate School of Medicine, 2-1 Seiryo-machi, Aoba-ku, Sendai 980-8575, Japan. E-mail: katagiri@mail.tains.tohoku.ac.jp.

This work was supported by a Grant-in-Aid for Young Scientists, B (16790503) (to T.O.), a Grant-in-Aid for Scientific Research (B2, 18390267) (to H.K.) from the Ministry of Education, Science, Sports, and Culture of Japan, and a Grant-in-Aid for Scientific Research (H16-genome-003) (to Y.O.) from the Ministry of Health, Labor, and Welfare of Japan. This work was also supported by grants from the 21st Century COE Program "CRESCENDO" (to H.K.) and "the Center for Innovative Therapeutic Development for Common Diseases" (to Y.O.) from the Ministry of Education, Science, Sports, and Culture of Japan.

Disclosure Statement: The authors have nothing to disclose.

References

1. **Krause DS, Theise ND, Collector MI, Henegariu O, Hwang S, Gardner R, Neutzel S, Sharkis SJ** 2001 Multi-organ, multi-lineage engraftment by a single bone marrow-derived stem cell. Cell 105:369–377
2. **Sata M, Saiura A, Kunisato A, Tojo A, Okada S, Tokuhisa T, Hirai H, Makuuchi M, Hirata Y, Nagai R** 2002 Hematopoietic stem cells differentiate into vascular cells that participate in the pathogenesis of atherosclerosis. Nat Med 8:403–409
3. **Takahashi T, Kalka C, Masuda H, Chen D, Silver M, Kearney M, Magner M, Isner JM, Asahara T** 1999 Ischemia- and cytokine-induced mobilization of bone marrow-derived endothelial progenitor cells for neovascularization. Nat Med 5:434–438
4. **Ferrari G, Cusella-De Angelis G, Coletta M, Paolucci E, Stornaiuolo A, Cossu G, Mavilio F** 1998 Muscle regeneration by bone marrow-derived myogenic progenitors. Science 279:1528–1530
5. **Orlic D, Kajstura J, Chimenti S, Jakoniuk I, Anderson SM, Li B, Pickel J, McKay R, Nadal-Ginard B, Bodine DM, Leri A, Anversa P** 2001 Bone marrow cells regenerate infarcted myocardium. Nature 410:701–705
6. **Okamoto R, Yajima T, Yamazaki M, Kanai T, Mukai M, Okamoto S, Ikeda Y, Hibi T, Inazawa J, Watanabe M** 2002 Damaged epithelia regenerated by bone marrow-derived cells in the human gastrointestinal tract. Nat Med 8:1011–1017
7. **Lee VM, Stoffel M** 2003 Bone marrow: an extra-pancreatic hideout for the elusive pancreatic stem cell? J Clin Invest 111:799–801
8. **Lechner A, Habener JF** 2003 Bone marrow stem cells find a path to the pancreas. Nat Biotechnol 21:755–756
9. **Tessem JS, DeGregori J** 2004 Roles for bone-marrow-derived cells in β-cell maintenance. Trends Mol Med 10:558–564
10. **Ianus A, Holz GG, Theise ND, Hussain MA** 2003 *In vivo* derivation of

glucose-competent pancreatic endocrine cells from bone marrow without evidence of cell fusion. J Clin Invest 111:843–850
11. Choi JB, Uchino H, Azuma K, Iwashita N, Tanaka Y, Mochizuki H, Migita M, Shimada T, Kawamori R, Watada H 2003 Little evidence of transdifferentiation of bone marrow-derived cells into pancreatic β cells. Diabetologia 46:1366–1374
12. Lechner A, Yang YG, Blacken RA, Wang L, Nolan AL, Habener JF 2004 No evidence for significant transdifferentiation of bone marrow into pancreatic β-cells *in vivo*. Diabetes 53:616–623
13. Taneera J, Rosengren A, Renstrom E, Nygren JM, Serup P, Rorsman P, Jacobsen SE 2006 Failure of transplanted bone marrow cells to adopt a pancreatic β-cell fate. Diabetes 55:290–296
14. Hess D, Li L, Martin M, Sakano S, Hill D, Strutt B, Thyssen S, Gray DA, Bhatia M 2003 Bone marrow-derived stem cells initiate pancreatic regeneration. Nat Biotechnol 21:763–770
15. Banerjee M, Kumar A, Bhonde RR 2005 Reversal of experimental diabetes by multiple bone marrow transplantation. Biochem Biophys Res Commun 328: 318–325
16. Izumida Y, Aoki T, Yasuda D, Koizumi T, Suganuma C, Saito K, Murai N, Shimizu Y, Hayashi K, Odaira M, Kusano T, Kushima M, Kusano M 2005 Hepatocyte growth factor is constitutively produced by donor-derived bone marrow cells and promotes regeneration of pancreatic β-cells. Biochem Biophys Res Commun 333:273–282
17. Li FX, Zhu JW, Tessem JS, Beilke J, Varella-Garcia M, Jensen J, Hogan CJ, DeGregori J 2003 The development of diabetes in E2f1/E2f2 mutant mice reveals important roles for bone marrow-derived cells in preventing islet cell loss. Proc Natl Acad Sci USA 100:12935–12940
18. Than S, Ishida H, Inaba M, Fukuba Y, Seino Y, Adachi M, Imura H, Ikehara S 1992 Bone marrow transplantation as a strategy for treatment of non-insulin-dependent diabetes mellitus in KK-Ay mice. J Exp Med 176:1233–1238
19. Mathews V, Hanson PT, Ford E, Fujita J, Polonsky KS, Graubert TA 2004 Recruitment of bone marrow-derived endothelial cells to sites of pancreatic β-cell injury. Diabetes 53:91–98
20. Aicher A, Heeschen C, Mildner-Rihm C, Urbich C, Ihling C, Technau-Ihling K, Zeiher AM, Dimmeler S 2003 Essential role of endothelial nitric oxide synthase for mobilization of stem and progenitor cells. Nat Med 9:1370–1376
21. Okabe M, Ikawa M, Kominami K, Nakanishi T, Nishimune Y 1997 'Green mice' as a source of ubiquitous green cells. FEBS Lett 407:313–319
22. Wang Z, Dohle C, Friemann J, Green BS, Gleichmann H 1993 Prevention of high- and low-dose STZ-induced diabetes with D-glucose and 5-thio-D-glucose. Diabetes 42:420–428
23. Ishihara H, Takeda S, Tamura A, Takahashi R, Yamaguchi S, Takei D, Yamada T, Inoue H, Soga H, Katagiri H, Tanizawa Y, Oka Y 2004 Disruption of the WFS1 gene in mice causes progressive β-cell loss and impaired stimulus-secretion coupling in insulin secretion. Hum Mol Genet 13:1159–1170
24. Ramiya VK, Maraist M, Arfors KE, Schatz DA, Peck AB, Cornelius JG 2000 Reversal of insulin-dependent diabetes using islets generated *in vitro* from pancreatic stem cells. Nat Med 6:278–282
25. Bonner-Weir S, Taneja M, Weir GC, Tatarkiewicz K, Song KH, Sharma A, O'Neil JJ 2000 *In vitro* cultivation of human islets from expanded ductal tissue. Proc Natl Acad Sci USA 97:7999–8004
26. Gao R, Ustinov J, Pulkkinen MA, Lundin K, Korsgren O, Otonkoski T 2003 Characterization of endocrine progenitor cells and critical factors for their differentiation in human adult pancreatic cell culture. Diabetes 52:2007–2015
27. Ema H, Suda T, Nakauchi H, Nakamura Y, Iwama A, Imagawa S, Akutsu M, Kano Y, Kato S, Yabe M, Yoshida M, Sakamoto S, Amemiya Y, Miura Y 1991 Multipotent and committed CD34+ cells in bone marrow transplantation. Jpn J Cancer Res 82:547–552
28. Tropepe V, Coles BL, Chiasson BJ, Horsford DJ, Elia AJ, McInnes RR, van der Kooy D 2000 Retinal stem cells in the adult mammalian eye. Science 287:2032–2036
29. Okano H 2002 Neural stem cells: progression of basic research and perspective for clinical application. Keio J Med 51:115–128
30. Trucco M 2005 Regeneration of the pancreatic β cell. J Clin Invest 115:5–12
31. Blyszczuk P, Wobus AM 2004 Stem cells and pancreatic differentiation *in vitro*. J Biotechnol 113:3–13
32. Dor Y, Brown J, Martinez OI, Melton DA 2004 Adult pancreatic β-cells are formed by self-duplication rather than stem-cell differentiation. Nature 429: 41–46
33. Georgia S, Bhushan A 2004 β Cell replication is the primary mechanism for maintaining postnatal β cell mass. J Clin Invest 114:963–968
34. Heissig B, Hattori K, Dias S, Friedrich M, Ferris B, Hackett NR, Crystal RG, Besmer P, Lyden D, Moore MA, Werb Z, Rafii S 2002 Recruitment of stem and progenitor cells from the bone marrow niche requires MMP-9 mediated release of kit-ligand. Cell 109:625–637
35. Menger MD, Vajkoczy P, Leiderer R, Jager S, Messmer K 1992 Influence of experimental hyperglycemia on microvascular blood perfusion of pancreatic islet isografts. J Clin Invest 90:1361–1369
36. Lammert E, Cleaver O, Melton D 2001 Induction of pancreatic differentiation by signals from blood vessels. Science 294:564–567
37. Nikolova G, Jabs N, Konstantinova I, Domogatskaya A, Tryggvason K, Sorokin L, Fassler R, Gu G, Gerber HP, Ferrara N, Melton DA, Lammert E 2006 The vascular basement membrane: a niche for insulin gene expression and β cell proliferation. Dev Cell 10:397–405
38. Otani A, Kinder K, Ewalt K, Otero FJ, Schimmel P, Friedlander M 2002 Bone marrow-derived stem cells target retinal astrocytes and can promote or inhibit retinal angiogenesis. Nat Med 8:1004–1010
39. Higashi Y, Kimura M, Hara K, Noma K, Jitsuiki D, Nakagawa K, Oshima T, Chayama K, Sueda T, Goto C, Matsubara H, Murohara T, Yoshizumi M 2004 Autologous bone-marrow mononuclear cell implantation improves endothelium-dependent vasodilation in patients with limb ischemia. Circulation 109:1215–1218

Endocrinology is published monthly by The Endocrine Society (http://www.endo-society.org), the foremost professional society serving the endocrine community.

Carboxy-terminal modulator protein induces Akt phosphorylation and activation, thereby enhancing antiapoptotic, glycogen synthetic, and glucose uptake pathways

Hiraku Ono, Hideyuki Sakoda, Midori Fujishiro, Motonobu Anai, Akifumi Kushiyama, Yasushi Fukushima, Hideki Katagiri, Takehide Ogihara, Yoshitomo Oka, Hideaki Kamata, Nanao Horike, Yasunobu Uchijima, Hiroki Kurihara and Tomoichiro Asano

Am J Physiol Cell Physiol 293:1576-1585, 2007. First published Jul 5, 2007;
doi:10.1152/ajpcell.00570.2006

Am J Physiol Cell Physiol 293: C1576–C1585, 2007.
First published July 5, 2007; doi:10.1152/ajpcell.00570.2006.

Carboxy-terminal modulator protein induces Akt phosphorylation and activation, thereby enhancing antiapoptotic, glycogen synthetic, and glucose uptake pathways

Hiraku Ono,[1]* Hideyuki Sakoda,[2]* Midori Fujishiro,[2] Motonobu Anai,[1] Akifumi Kushiyama,[2] Yasushi Fukushima,[2] Hideki Katagiri,[3] Takehide Ogihara,[3] Yoshitomo Oka,[3] Hideaki Kamata,[5] Nanao Horike,[4] Yasunobu Uchijima,[4] Hiroki Kurihara,[4] and Tomoichiro Asano[5]

[1]*Department of Endocrinology and Metabolism, Institute for Adult Disease, Asahi Life Foundation, Chiyoda-ku, Tokyo;* [2]*Department of Internal Medicine, Graduate School of Medicine, University of Tokyo, Bunkyo-ku, Tokyo;* [3]*Division of Advanced Therapeutics for Metabolic Diseases, Department of Translational Research, Tohoku University, Graduate School of Medicine, Aoba-ku, Sendai, Miyagi;* [4]*Department of Physiological Chemistry and Metabolism, Graduate School of Medicine, University of Tokyo, Bunkyo-ku, Tokyo; and* [5]*Department of Medical Science, Graduate School of Medicine, University of Hiroshima, Minami-ku, Hiroshima City, Hiroshima, Japan*

Submitted 9 November 2006; accepted in final form 3 July 2007

Ono H, Sakoda H, Fujishiro M, Anai M, Kushiyama A, Fukushima Y, Katagiri H, Ogihara T, Oka Y, Kamata H, Horike N, Uchijima Y, Kurihara H, Asano T. Carboxy-terminal modulator protein induces Akt phosphorylation and activation, thereby enhancing antiapoptotic, glycogen synthetic, and glucose uptake pathways. *Am J Physiol Cell Physiol* 293: C1576–C1585, 2007. First published July 5, 2007; doi:10.1152/ajpcell.00570.2006.—Carboxy-terminal modulator protein (CTMP) was identified as binding to the carboxy terminus of Akt and inhibiting the phosphorylation and activation of Akt. In contrast to a previous study, we found CTMP overexpression to significantly enhance Akt phosphorylation at both Thr^{308} and Ser^{473} as well as the kinase activity of Akt, while phosphatidylinositol 3-kinase (PI3-kinase) activity was unaffected. Translocation of Akt to the membrane fraction was also markedly increased in response to overexpression of CTMP, with no change in the whole cellular content of Akt. Furthermore, the phosphorylations of GSK-3β and Foxo1, well-known substrates of Akt, were increased by CTMP overexpression. On the other hand, suppression of CTMP with small interfering RNA partially but significantly attenuated this Akt phosphorylation. The cellular activities reportedly mediated by Akt activation were also enhanced by CTMP overexpression. UV-B-induced apoptosis of HeLa cells was significantly reversed not only by overexpression of the active mutant of Akt (myr-Akt) but also by that of CTMP. Increases in glucose transport activity and glycogen synthesis were also induced by overexpression of either myr-Akt or CTMP in 3T3-L1 adipocytes. Taking these results into consideration, it can be concluded that CTMP induces translocation of Akt to the membrane and thereby increases the level of Akt phosphorylation. As a result, CTMP enhances various cellular activities that are principally mediated by the PI3-kinase/Akt pathway.

phosphatidylinositol 3-kinase

SERINE/THREONINE KINASE Akt has been established as one of the most important molecules in intracellular signaling cascades of growth hormones including insulin (9, 13, 22, 26, 44, 51). Its activation mechanisms have been clarified to some extent in recent years (1, 7): tyrosine kinase-type growth hormone receptors activate phosphatidylinositol 3-kinase (PI3-kinase), which generates 3-phosphoinositides on the plasma membrane. Akt is then recruited to the membrane through the binding of its PH domain and these 3-phosphoinositides (6, 19). When Akt reaches the membrane, two phosphorylation sites (Thr^{308} and Ser^{473}) of Akt are phosphorylated by phosphoinositide-dependent kinase (PDK)-1 (45, 46) and by PDK-2 (18, 28, 38, 39, 50), respectively. Recent reports have indicated that PDK-2 is very likely to be the mammalian target of rapamycin (mTOR)-Rictor complex (24, 43). Once phosphorylated at both sites, Akt is fully activated.

Recently, several proteins that modify the Akt activation state via direct binding to Akt (2, 4, 14, 34, 40) have been identified. Among them, carboxy-terminal modulator protein (CTMP) (23, 34) was reported to bind to the carboxy-terminal regulatory domain of Akt and to inhibit its activation. In addition, it was shown that stable CTMP overexpression in AKT8 cells inhibits tumor growth in nude mice. However, Akt is related not only to cell proliferation but also to antiapoptosis (12, 29, 35) and glucose metabolic processes such as glycogen synthesis, gluconeogenesis, glycolysis, and glucose uptake (16, 21, 25, 32, 47, 48, 51). The effects of CTMP on insulin signaling and on glucose metabolism have not previously been examined. Therefore, the initial aim of this study was to determine whether CTMP is a molecule involved in the insulin sensitivity of glucose metabolic processes, via its effect on Akt activity.

However, in our study, overexpression of CTMP was demonstrated to obviously enhance Akt phosphorylation regardless of whether a transient or a stable expression system was used. To our surprise, this is quite the opposite of previously reported results. When endogenous CTMP was suppressed by small interfering RNA (siRNA), Akt phosphorylations were reduced. Moreover, several cellular functions downstream from Akt, such as antiapoptotic and glucose metabolic processes, were shown to be enhanced by CTMP. We thus conclude that CTMP is a positive regulator of Akt.

* H. Ono and H. Sakoda contributed equally to this work.

Address for reprint requests and other correspondence: T. Asano, Dept. of Medical Science, Graduate School of Medicine, Univ. of Hiroshima, 1-2-3 Kasumi, Minami-ku, Hiroshima City, Hiroshima 734-8551, Japan (e-mail: tasano@hiroshima-u.ac.jp).

The costs of publication of this article were defrayed in part by the payment of page charges. The article must therefore be hereby marked "*advertisement*" in accordance with 18 U.S.C. Section 1734 solely to indicate this fact.

MATERIALS AND METHODS

Antibodies and immunoblotting. Anti-CTMP antibody was raised by immunizing rabbits with the keyhole limpet hemocyanin-conjugated 17 carboxy-terminal amino acids of CTMP and affinity purified on Affi-Gel-10 (Bio-Rad, Hercules, CA) columns to which the corresponding peptide had been coupled. The animal protocol was approved by the University of Tokyo Ethics Committee for Animal Experiments and strictly adhered to the guidelines for animal experiments of the University of Tokyo. Anti-Akt antibody was described previously (37). Anti-phospho-Thr^{308} Akt, anti-phospho-Ser^{473} Akt, anti-phospho-Ser^{9} GSK-3β, and anti-phospho-Ser^{256} Foxo1 were purchased from Cell Signaling Technology (Beverly, MA). Anti-phosphotyrosine antibody (4G10) was purchased from Upstate Biotechnology (Lake Placid, NY). Immunoblotting was carried out with enhanced chemiluminescence (ECL Detection Kit, Amersham), and representative blots were obtained by exposing the films. The bands were quantitatively analyzed with Molecular Imager FX (Bio-Rad) without exposure of the films.

DNA constructs, expression vectors, and adenoviruses. Complete cDNA of human CTMP was amplified by PCR from a cDNA library of HeLa cells with a primer set based on the reported sequence (34). Amino-terminal FLAG tag was added, also by PCR. All the sequences were confirmed with a CEQ-2000XL DNA sequencer (Beckman Coulter, Tokyo, Japan). To prepare the plasmid expression vector, cDNA was subcloned into pcDNA3.1(−) (Invitrogen, Carlsbad, CA). To prepare the adenovirus for CTMP expression, the DNA construct was subcloned into a pAdexCAwt cosmid cassette and transfected with the parental viral genome into HEK293 cells as described previously (27). Adenovirus vectors for carboxy-terminally myc-tagged wild-type (WT) Akt, carboxy-terminally myc-tagged myr-Akt, and *Escherichia coli* β-galactosidase (LacZ) were described previously (27, 52). Adenoviruses were concentrated and purified by ultracentrifugation in a CsCl gradient as described previously (33).

Cell culture, adenoviral infection, and serum starvation. COS-1, HepG2, HeLa, and NIH3T3 cells were cultured in DMEM containing 4.5 g/l glucose, penicillin-streptomycin (Pen/Strep), and 10% fetal

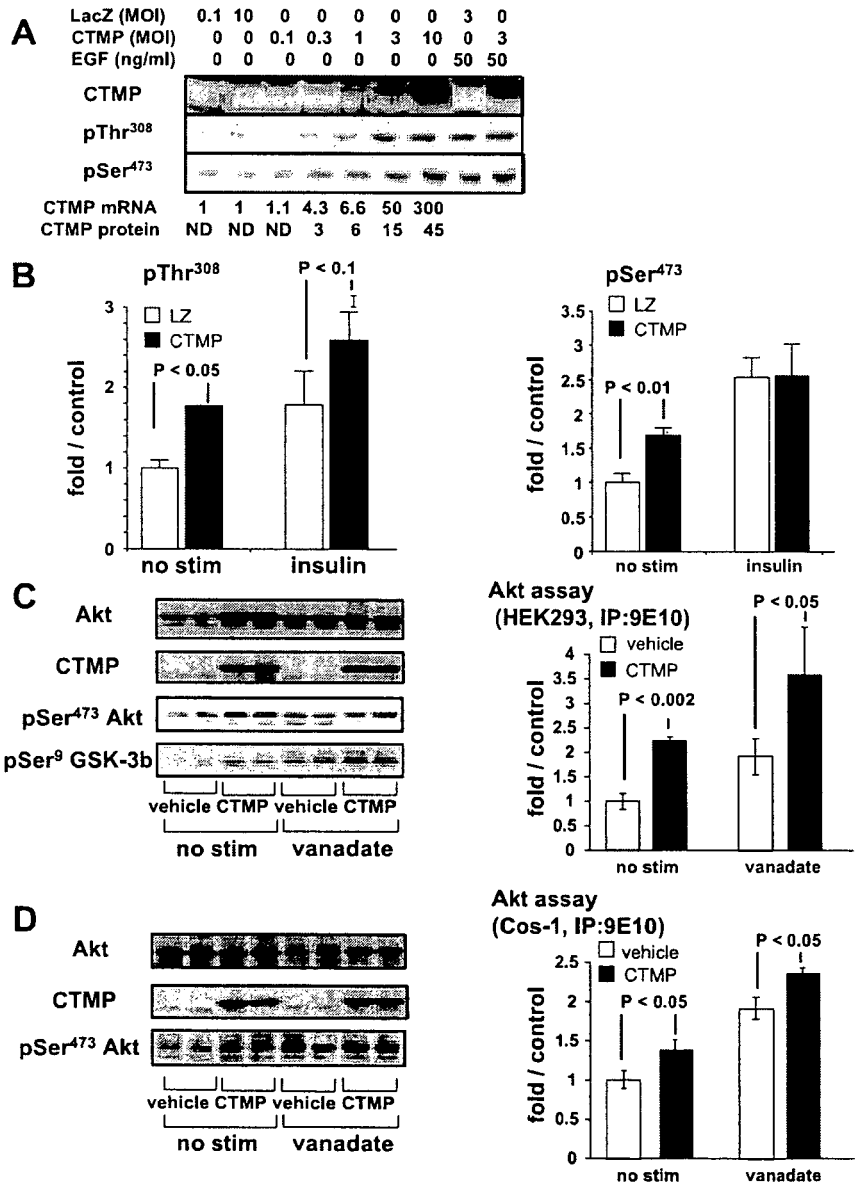

Fig. 1. Effects of transiently overexpressed carboxy-terminal modulator protein (CTMP) on Akt phosphorylation and activation. *A*: COS-1 cells were infected with various titers [multiplicity of infection (MOI) = 0.1–10] of LacZ or CTMP adenovirus. Phosphorylations of endogenous Akt at Thr^{308} or Ser^{473} without or with 50 ng/ml EGF stimulation were assayed by Western blotting with phospho-specific antibodies. Representative bands from duplicate experiments are shown. The multiplicity of CTMP expression at its mRNA level or protein level was assayed, and is shown at *bottom*. The protein level is indicated by inequality, because our antibody could not detect endogenous CTMP [not detected (ND)]. LacZ did not influence Akt phosphorylations, regardless of its MOI or EGF stimulation. CTMP enhanced these phosphorylations in a dose-dependent manner in the nonstimulated (basal) state. CTMP did not suppress Akt phosphorylations even when the cells were stimulated with EGF. *B*: HepG2 cells were infected with CTMP or LacZ (LZ) with adenoviral vectors. Phosphorylations of endogenous Akt at Thr^{308} (*left*) or Ser^{473} (*right*) in HepG2 cells without (no stim) or with 100 nM insulin stimulation were assayed as in *A* and quantified in experiments performed in triplicate. Values are mean ± SE fold increase over LacZ without insulin. The enhancing effect of CTMP on Akt phosphorylation was also observed in HepG2 cells. *C*: Akt phosphorylation and kinase activity were assayed in HEK293 cells. HEK293 cells were transfected with the expression vector containing CTMP cDNA and were coexpressed with wild-type Akt with adenoviral vectors. *Left*: overexpression of CTMP and CTMP-induced increases in phosphorylations of Akt and GSK-3β. *Right*: CTMP-induced increase in Akt kinase activity with or without vanadate stimulation. Values are mean ± SE fold increase over vehicle without stimulation. ANOVA confirmed the significance of the enhancing effect of CTMP on Akt activity. *D*: Akt phosphorylation and kinase activity were assayed in COS-1 cells transfected with the expression vector containing CTMP cDNA. *Right*: overexpression of CTMP and CTMP-induced increases in phosphorylations of Akt. *Left*: CTMP-induced increase in Akt kinase activity with or without vanadate stimulation. Values are mean ± SE fold increase over vehicle without stimulation. ANOVA confirmed the significance of the enhancing effect of CTMP on Akt activity. CTMP or vehicle was coexpressed with wild-type Akt with adenoviral vectors. The effect of CTMP on Akt phosphorylations was enhanced. IP, immunoprecipitation.

calf serum (FCS) under a 5% CO_2 atmosphere at 37°C. Adenoviral infection and serum starvation were carried out simultaneously for these cell types 24 h before the following experiments, i.e., the cells were incubated with adenovirus for 1 h, washed once with serum-free DMEM containing 0.2% BSA, and then incubated with that serum-free medium for 24 h. NIH3T3 cells stably transfected with CTMP constructs (pcDNA) were selected and maintained in DMEM containing 500 mg/l Geneticin. 3T3-L1 adipocytes were prepared from 3T3-L1 fibroblasts as described previously (41). Four days after the induction of differentiation, at which time >90% of the 3T3-L1 cells expressed the adipocyte phenotype, viral infection of these cells was carried out. Serum starvation of 3T3-L1 adipocytes is described below.

Plasmid transfection and Akt kinase assay. COS-1 cells or HEK293 cells were maintained in DMEM supplemented with 10% FCS (Life Technologies) and 50 U/ml Pen/Strep (GIBCO). Transfections were performed with the calcium phosphate technique (34). To obtain a cell line stably overexpressing CTMP, selection was carried out with G-418 after plasmid transfection.

After cells were first serum starved for 12 h in serum-free DMEM, they were stimulated with 100 μM pervanadate for 10 min at 37°C. Next, the cells were lysed in lysis buffer [mM: 50 Tris·HCl (pH 7.5), 150 NaCl, 1 EDTA, 1 EGTA, 2.5 sodium pyrophosphate, 1 sodium orthovanadate, 1 β-glycerophosphate, and 0.2 PMSF, with 1% Triton X-100] and centrifuged. The supernatants were then immunoprecipitated with anti-myc antibodies and protein G Sepharose beads. The immunoprecipitants were washed three times with lysis buffer and twice with kinase assay buffer [mM: 50 Tris·HCl (pH 7.5), 10 $MgCl_2$, 1 EGTA, and 1 dithiothreitol]. Beads were resuspended in 45 μl of kinase assay buffer, and reactions were initiated by the addition of 5 μl of an ATP mixture containing 5 μM nonradioactive ATP, 2 μCi of [γ-^{32}P]ATP (4,000 Ci/mmol), and 5 μM Crosstide and then incubated for 30 min at 30°C. The kinase reaction mixture was spotted onto a P81 filter (Whatman), the filters were washed three times with 0.5% (wt/vol) orthophosphoric acid, and the radioactivity remaining on the filters was measured with a BAStation2000 (Fujifilm).

Adenoviral gene transfer and Akt kinase assay. COS-1 cells in 10-cm dishes, 24 h after serum starvation and viral infection [multiplicity of infection (MOI) 3], were stimulated without or with 50 ng/ml EGF for 10 min, washed once with ice-cold PBS, and lysed with 1 ml/dish of lysis buffer from an Akt kinase assay kit (Cell Signaling Technology). Insoluble materials were eliminated by centrifugation, and 200 μl of the supernatants was immunoprecipitated with 10 μl of immobilized Akt monoclonal antibody. Subsequent steps were carried out according to the manufacturer's instructions.

RNA silencing of CTMP in HeLa cells. HeLa cells were seeded at 1×10^4 cells/well onto 24-well plates. At 24 h after seeding, siRNAs were transfected, i.e., 0.25 μg of siRNA of CTMP (target sequence: AAGCATGAAGAATAAATACAT) or lamin (control siRNA, target sequence: AACTGGACTTCCAGAAGAACA), 1.5 μl of RNAiFect transfection reagent (Qiagen, Tokyo, Japan), and DMEM containing 10% FCS (total 100 μl/well) were mixed, incubated for 10 min, and dropped into each well. At 36 h after transfection, cells were serum starved. After 12 h of starvation, the cells were stimulated without or with 1 μM insulin for 15 min and lysed with the lysis buffer from an RNAqueous kit (Ambion, Austin, TX) or Laemmli buffer.

Total RNA was purified with the RNAqueous kit according to the manufacturer's instructions. RNA was then reverse transcribed with Superscript III (Invitrogen). cDNA levels of CTMP and GAPDH (internal standard) were quantified with LightCycler and DNA Master SYBR Green I (Roche Diagnostics, Tokyo, Japan). The primer sequences used were TCTGAGGAAGTCATTCTTAAG and CTCATCAACACTCTGAACATT for CTMP and GAAGGTGAAGGTCGGAGTC and GAAGATGGTGATGGGATTTC for GAPDH.

Subcellular fractionation. In a 15-cm dish, COS-1 cells (24 h after virus infection at MOI 3) were washed with PBS and scraped off into 2 ml of HES (mM: 20 HEPES pH 7.4, 1 EDTA, 250 sucrose) containing protease/phosphatase inhibitors (mM: 1 PMSF, 1 orthovanadate, 40 β-glycerophosphate, 50 NaF). The cell suspension was homogenized with 10 strokes of a Teflon homogenizer and centrifuged at 600 *g* for 15 min to eliminate the nuclear fraction. The supernatant was ultracentrifuged at 250,000 *g* for 90 min, and the pellet was rinsed once with HES and lysed with 100 μl of lysis buffer (mM: 50 Tris pH 7.4, 100 NaCl, 10 EDTA, with 10% glycerol and 1% Nonidet P-40) containing protease/phosphatase inhibitors. The lysate was then recentrifuged at 15,000 *g* for 15 min to eliminate the cytoskeletal fraction. The supernatant was taken as the membrane fraction.

PI3-kinase activity assay. COS-1 cells in 12-well culture plates, 24 h after serum starvation and viral infection (MOI 3), were stimulated

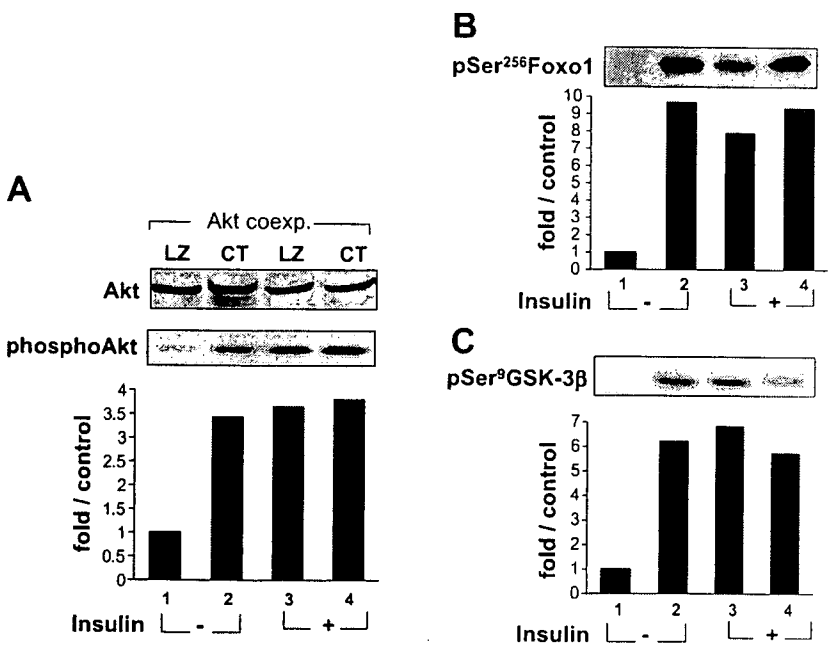

Fig. 2. Positive effect of CTMP on Foxo1 and GSK-3β phosphorylations in HeLa cells. HeLa cells were infected with adenovirus to overexpress LacZ (LZ) or CTMP (CT) with wild-type Akt and stimulated without or with 100 nM insulin for 15 min. *A*: overexpressed Akt was confirmed with Western blotting using anti-myc antibody (*top*). Phosphorylation of overexpressed Akt at Thr^{308} was assayed by Western blotting (*middle*), and phosphorylation levels were quantified (*bottom*). *B* and *C*: phosphorylation of Ser^{256} of Foxo1 and Ser^{9} of GSK-3β were assayed by Western blotting with the respective phospho-specific antibodies (*B* and *C*, *top*, respectively), and phosphorylation levels were quantified (*B* and *C*, *bottom*, respectively).

without or with 50 ng/ml EGF or 100 nM sodium orthovanadate for 10 min, washed once with ice-cold PBS, and lysed with lysis buffer (PBS containing 1% Nonidet P-40, 0.35 mg/ml PMSF, and 100 mM sodium orthovanadate). Insoluble materials were eliminated by centrifugation, and the supernatants were immunoprecipitated with anti-phosphotyrosine antibodies and protein G Sepharose. The PI3-kinase activity in the immunoprecipitants was measured as described previously (27).

UV-B irradiation and MTT assay of HeLa cells. HeLa cells were plated onto a 96-well culture plate at a density of 1×10^4 cells/well. At 24 h after seeding, the cells were infected with adenoviruses at an MOI of 3 for 1 h. After infection, the cells were washed once with serum-free DMEM containing 0.2% BSA and incubated in the same medium for 12 h. The medium was then replaced with PBS, and the plate was irradiated with UV-B (wavelength = 312 nm, energy = 8 mW/cm^2; DT-20MCP UV illuminator, ATTO, Tokyo, Japan) for 6 min from the bottom face of the plate. The PBS was then replaced with 100 μl of serum-free DMEM containing 0.2% BSA, and the cells were incubated at 37°C. At 8 h after the irradiation, 10 μl of 12 mM 4,5-dimethylthiazol-2-yl-2,5-diphenyltetrazolium bromide (MTT) solution in PBS was added to each well, and the 37°C incubation was continued for 4 h. One hundred microliters of 10 mM HCl containing 10% SDS was added to each well. After vigorous mixing of each well by pipetting, the plate was incubated at 37°C for 2 h, each well was pipetted again, and absorbance at 570 nm was measured with a microplate reader. Each treatment combination (virus and UV irradiation) was examined four times (n = 4).

2-Deoxyglucose uptake assay. 3T3-L1 adipocytes in 24-well culture plates were infected with adenovirus at an MOI of 100. At 45 h after infection, the cells were washed once with DMEM containing 0.2% BSA and incubated in that medium for 3 h for serum starvation.

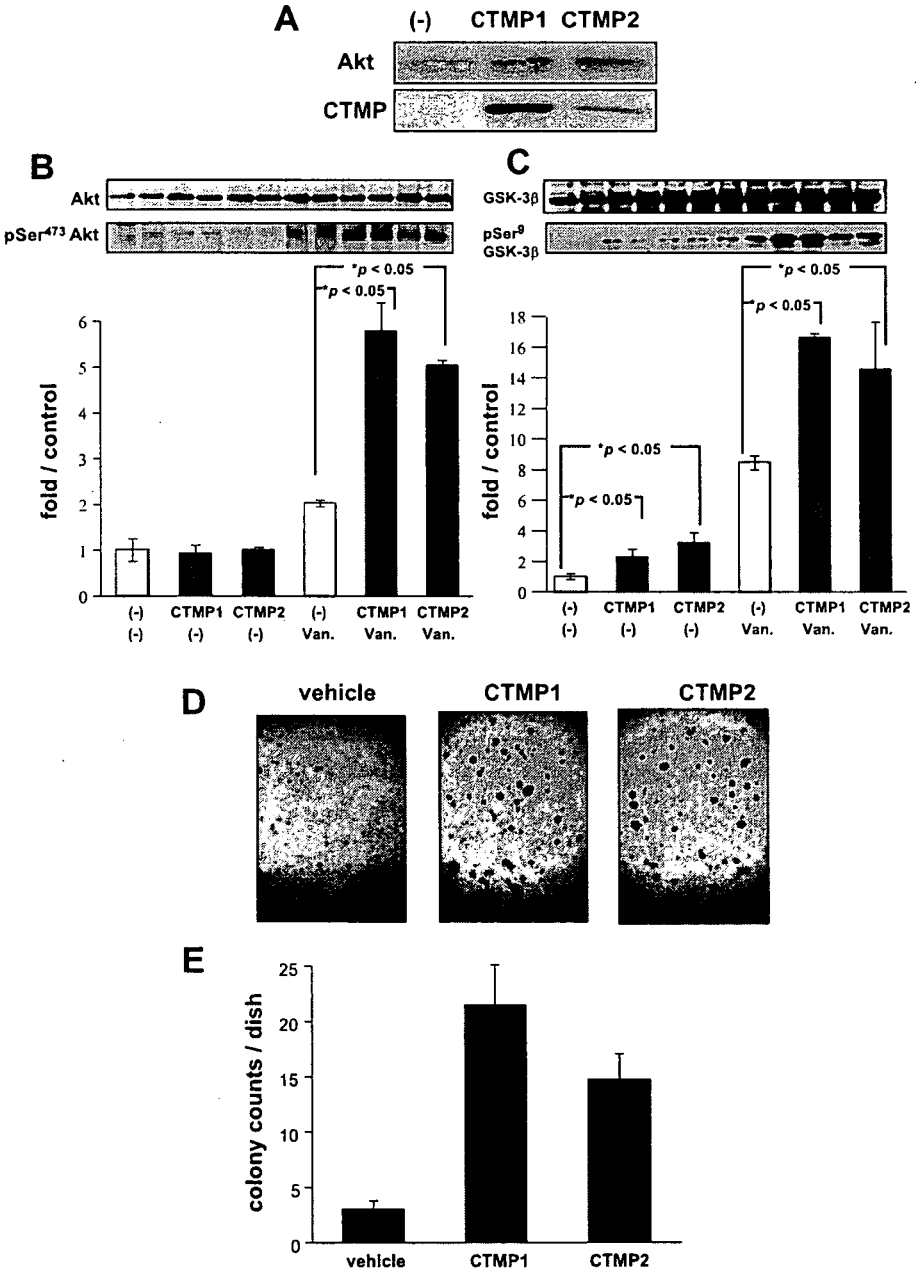

Fig. 3. Effects of stably overexpressed CTMP on Akt and GSK-3β phosphorylations in NIH3T3 cells. NIH3T3 cells were transfected with the expression vector containing CTMP cDNA and subjected to G-418 selection. Control cells were transfected with the expression vector alone, i.e., without CTMP cDNA. *A*: 2 representative cell lines (CTMP1 and CTMP2) overexpressing CTMP were isolated (*bottom*), and the absence of significant alteration of Akt expression was confirmed (*top*). *B* and *C*: Akt (*B*) and GSK-3β (*C*) phosphorylations were examined in the control and 2 CTMP overexpressing cell lines in the absence or presence of vanadate stimulation (Van). *D* and *E*: soft agar assays demonstrating transformation of NIH3T3 fibroblasts by CTMP. For the soft agar assay, NIH3T3 cells stably transfected with CTMP constructs were trypsinized, suspended in DMEM containing 0.3% agar and 20% fetal calf serum, and plated onto a bottom layer containing 0.6% agar. Cells were plated at a density of 2×10^4 cells per 3.5-cm dish. Colonies >0.5 mm in diameter were counted after 14 days (*E*). Four independent experiments were performed, and similar results were obtained.

Next, glucose-free incubation was performed for 45 min in Krebs-Ringer phosphate buffer (8). Cells were then incubated with 0, 1, 10, or 100 nM insulin for 15 min, and 2-deoxy-D-[^{3}H]glucose uptake during the subsequent 4 min was measured as described previously (3). Each treatment combination (virus and insulin) was examined twice.

Glycogen synthesis assay. 3T3-L1 adipocytes in 24-well culture plates were infected with adenovirus at an MOI of 100 in DMEM containing 4.5 g/l glucose and 10% FCS. At 40 h after infection, the cells were washed once with serum-free DMEM containing 1 g/l glucose and 0.2% BSA and then incubated with the same medium for 5 h. The cells were then incubated with 200 μl of the same medium containing 1.5 μCi/ml of D-[U-^{14}C]glucose (230–370 mCi/mmol) and stimulated with 0, 0.1, 1, or 100 nM insulin for 3 h. After insulin stimulation, the cells were washed twice with ice-cold PBS and incubated with 200 μl of 10 N KOH at 4°C for 3 h. The cells were then scraped off, collected, and boiled with 2 mg of glycogen for 30 min. The lysate was mixed with 800 μl of ethanol and incubated at −20°C overnight. Tubes were centrifuged at 15,000 rpm for 20 min, and the supernatant was discarded. The glycogen pellets were rinsed once with 80% ethanol, dissolved in 200 μl of water, mixed with 800 μl of ethanol, and incubated again at −20°C overnight. The tubes were centrifuged, the pellets were dissolved in 200 μl of 0.1 N HCl and mixed with ACS II (Amersham Biosciences, Piscataway, NJ), and the incorporated ^{14}C was quantified with a liquid scintillator. Each treatment combination (virus and insulin) was examined twice.

Statistical analysis. Figures 1–8 show means ± SE. To analyze the results of the experiments, Student's unpaired *t*-test or two-way ANOVA with replication was used to demonstrate significant differences. With two-way ANOVA, mainly viral and growth hormone stimulation factors were assessed.

RESULTS

Transient CTMP overexpression enhanced Akt phosphorylation and activation in COS-1, HepG2, HEK293, and HeLa cells under both unstimulated and stimulated conditions. We created an expression vector as well as an adenovirus to express amino-terminally FLAG-tagged CTMP in cultured cells. In our subsequent experiments, COS-1, HeLa, and HepG2 cells and 3T3-L1 adipocytes were infected with this virus. We confirmed an ~22-kDa single band in the samples from these infected cells, using either anti-FLAG antibody or anti-CTMP antibody (Fig. 1*A*, *top*).

To investigate whether CTMP influences the phosphorylation state of Akt, we infected COS-1 cells with various titers of CTMP or LacZ (control) virus at an MOI of 3 and evaluated phosphorylations of Akt at Thr^{308} and Ser^{473} by immunoblotting with phospho-specific antibodies. As shown in Fig. 1*A*, CTMP enhanced endogenous Akt phosphorylations at both sites, in a viral dose-dependent manner, in the basal state, while control LacZ virus had no effect. The maximal level of Akt phosphorylation by CTMP overexpression was comparable with that induced by EGF stimulation. EGF stimulation had a small additional effect on Akt phosphorylation in CTMP-overexpressing cells (Fig. 1*A*, *right 2 lanes*), suggesting that high CTMP expression could induce nearly maximal Akt phosphorylation.

Subsequently, to confirm this phenomenon, we investigated the effects of CTMP overexpression on Akt phosphorylation by expressing CTMP in other types of cultured cells such as HepG2 and HeLa cells and 3T3-L1 adipocytes. In HepG2 cells, which are insulin-sensitive cells, CTMP produced a similar enhancement of Akt phosphorylation (Fig. 1*B*). Infection of HeLa cells produced a similar result (data not shown).

To rule out the possibility that the difference in overexpression systems between plasmid transfection and adenoviral gene transfer was responsible for the different results, CTMP was transiently overexpressed in HEK293 and COS-1 cells (Fig. 1, *C* and *D*, respectively) with an expression plasmid containing CTMP cDNA and the calcium phosphate method. In HEK293 cells, CTMP overexpression increased Akt phosphorylation as shown by immunoblotting with phospho-specific antibodies under both basal and vanadate-treated conditions (Fig. 1*C*, *left*). The phosphorylation of GSK-3β was also markedly increased by CTMP overexpression. Indeed, Akt kinase activity was increased by CTMP overexpression under both basal and vanadate-treated conditions (Fig. 1*C*, *right*). Very similar effects were also observed in COS-1 cells transfected with the CTMP expression plasmid (Fig. 1*D*). These results strongly suggest that CTMP overexpression increases Akt phosphory-

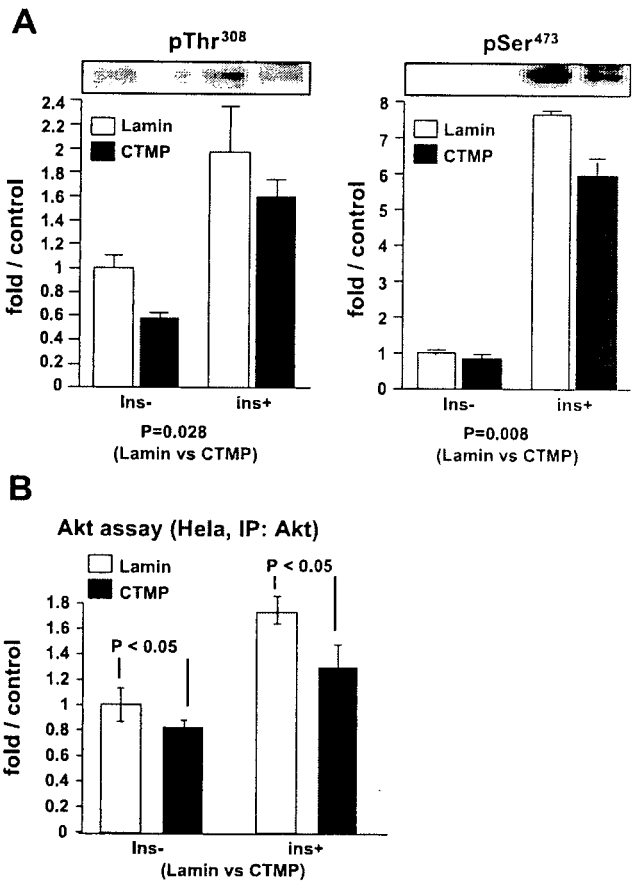

Fig. 4. CTMP small interfering RNA (siRNA) in HeLa cells. HeLa cells were transfected with siRNA of lamin (control) or CTMP, and Akt phosphorylations were measured 48 h after transfection. *A*: Akt phosphorylations at Thr^{308} and Ser^{473} were assayed by Western blotting, and representative bands are shown at *top* (Thr^{308}, *left*; Ser^{473}, *right*). Phosphorylation levels at Thr^{308} and Ser^{473} were quantified in experiments conducted in triplicate, and mean ± SE fold increases over LacZ without insulin are shown at *bottom*. Akt phosphorylations at Thr^{308} and Ser^{473} were significantly decreased by siRNA of CTMP. *B*: Akt kinase activities were quantified in experiments conducted in triplicate, and values are mean ± SE fold increases over LacZ without insulin.

lation and activity, irrespective of the transfection method or cell types.

CTMP expression induced phosphorylations of Foxo1 and GSK-3β in HeLa cells. In the following experiments, we investigated the effects of CTMP on signals downstream from Akt. First, we examined phosphorylations of well-known Akt substrates, Foxo1(5, 31) and GSK-3β (11, 49), using their respective phospho-specific antibodies. Insulin induced both Foxo1 and GSK-3β phosphorylation in HeLa cells overexpressing Akt (Fig. 2, *lane 3*). Co-overexpression of CTMP enhanced the phosphorylation of both Foxo1 and GSK-3β in the basal state, compared with that of LacZ (Fig. 2, *lane 2*), although no significant difference was observed in the presence of insulin stimulation.

Stable overexpression of CTMP enhances phosphorylations of Akt and GSK-3β in NIH3T3 cells. To exclude the possibility that the difference between stable and transient overexpressions is responsible for the different results, CTMP was stably overexpressed in NIH3T3 cells by expression plasmid transfection followed by G-418 selection. As shown in Fig. 3*A*, two cell lines overexpressing CTMP (CTMP1 showing higher expression level than CTMP2) were prepared, and the expression level of Akt was confirmed to be unchanged. While basal Akt phosphorylation was not significantly altered in either CTMP-overexpressing cell line (Fig. 3*B*, *left 3 lanes*), Akt phosphorylation in response to vanadate stimulation was markedly enhanced in the CTMP-overexpressing cells (Fig. 3*B*, *right 3 lanes*). The phosphorylation of GSK-3β was also demonstrated to be significantly increased by stable CTMP overexpression under both unstimulated and vanadate-stimulated conditions (Fig. 3*C*). These results indicate that stable overexpression of CTMP increases Akt activity under vanadate-stimulated conditions.

siRNA of CTMP inhibited Akt phosphorylation. Next, we suppressed endogenous CTMP expression with siRNA to examine its physiological functions. The mRNA level of CTMP was determined by real-time PCR and standardized with that of GAPDH. siRNA decreased CTMP transcription to approximately one-fifth of that in HeLa cells transfected with lamin siRNA [lamin 1.00 ± 0.27, CTMP 0.21 ± 0.01 (arbitrary units); $P = 0.002$], although inhibition of CTMP protein expression could not be examined because the CTMP antibody was not sufficiently sensitive to detect endogenous CTMP protein in HeLa cells. Under these conditions, phosphorylations of Akt were partially but significantly suppressed at both Thr^{308} and Ser^{473} sites by CTMP siRNA to a greater extent than by lamin siRNA, as shown in Fig. 4*A*, *top*. Akt kinase activity was also slightly but significantly suppressed by treatment with CTMP siRNA (Fig. 4*B*).

CTMP enhanced membrane localization of Akt without affecting PI3-kinase activity. To elucidate the mechanism underlying the positive effect of CTMP on Akt activation, we prepared the membrane fraction of COS-1 cells overexpressing CTMP or control LacZ by adenoviral gene transfer at an MOI of 3. As shown in Fig. 5*A*, *left*, immunoblotting revealed that overexpression of CTMP markedly increased the amount of Akt in the membrane fraction in the basal state and also slightly but significantly increased that in the EGF-stimulated state.

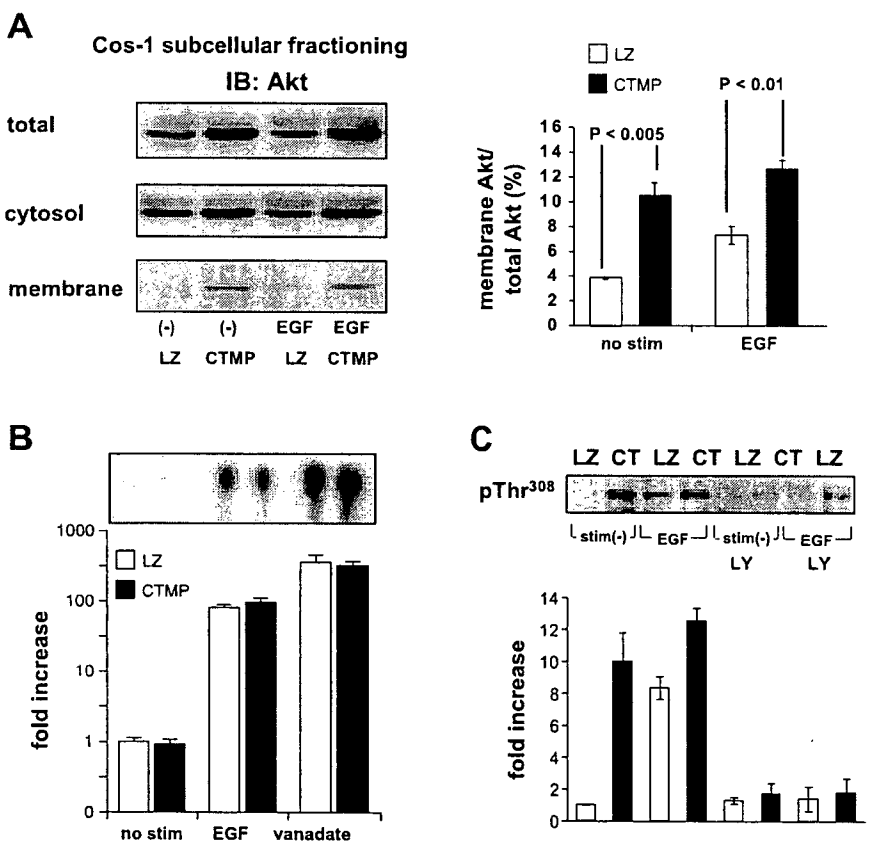

Fig. 5. Mechanisms of CTMP effect on Akt. *A*: COS-1 membrane fraction was purified with ultracentrifugation and then electrophoresed and immunoblotted (IB) with anti-Akt antibody. CTMP markedly increased membrane-localized Akt, especially in the basal state. The calculated ratio of membrane Akt to total Akt is shown at *right*. The experiment was done in triplicate. The graph shows means ± SE, and 1 band representative of the 3 is presented. *B*: COS-1 cells were stimulated without or with 50 ng/ml EGF or 100 nM orthovanadate, and anti-phosphotyrosine-immunoprecipitated phosphatidylinositol 3-kinase (PI3-kinase) activity in the cell lysate was assayed. The graph shows the fold increase ± SE over LacZ without stimulation on a logarithmic scale. CT, CTMP. Each experiment was done 3 times, and 1 spot representative of the 3 is shown at *top*. PI3-kinase activity was unchanged by CTMP expression, regardless of stimulation. *C*: COS-1 expressing LacZ or CTMP (CT) were stimulated without or with EGF for 10 min and then incubated without or with 20 nM LY-294002 (LY) for 2 min. Akt phosphorylations at Thr^{308} were quantified in experiments conducted in triplicate, and representative bands are shown at *top*. The graph shows mean ± SE fold increases over LacZ without insulin. The enhancing effect of CTMP on Akt phosphorylations was reversed within 2 min of LY-294002 incubation.

The ratio of membrane Akt to total Akt was calculated and is shown in Fig. 5*A*, *right*.

To exclude the possibility that the effects of CTMP on Akt are mediated by PI3-kinase activation that is upstream from Akt, we assayed the PI3-kinase activity of anti-phosphotyrosine immunoprecipitants from LacZ- or CTMP-expressing COS-1 cells. As shown in Fig. 5*B*, PI3-kinase activity did not differ between samples from LacZ-expressing cells and those expressing CTMP.

However, it was shown that treatment with LY-294002 obviously attenuated the Akt phosphorylation induced by either CTMP overexpression or EGF stimulation within 2 min (Fig. 5*C*). Thus it is likely that CTMP does enhance Akt phosphorylation, but at least basal level PI3-kinase activity is necessary.

CTMP expression with Akt rescued HeLa cells from UV-B irradiation-induced apoptosis. One of the well-known functions of Akt is antiapoptosis. Therefore, we investigated whether CTMP overexpression produces an antiapoptotic effect on cultured cells. HeLa cells, 12 h after adenoviral infection, were irradiated with UV-B. Cellular viability after irradiation was assayed with the MTT assay. As shown in Fig. 6, expression of CTMP alone tended to increase cellular viability

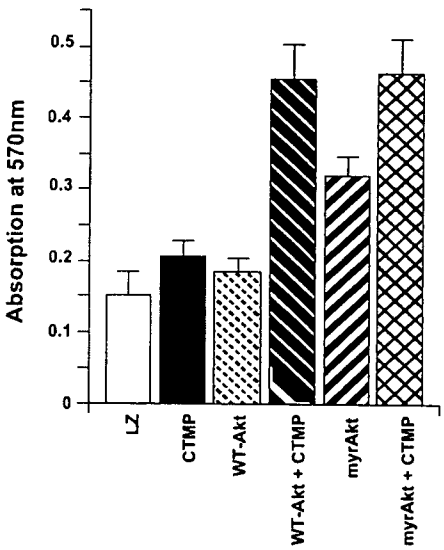

comparison		p value
LZ	CTMP	0.0002
LZ	WT-Akt	NS
LZ	WT-Akt + CTMP	<0.0001
LZ	myrAkt	0.0002
CTMP	WT-Akt + CTMP	0.0002
WT-Akt	WT-Akt + CTMP	<0.0001
myrAkt	myrAkt + CTMP	0.0514

Fig. 6. 4,5-Dimethylthiazol-2-yl-2,5-diphenyltetrazolium bromide (MTT) assay of UV-B-irradiated HeLa cells. HeLa cells in 96-well culture plates were infected with adenovirus in 6 combinations: LacZ (LZ), CTMP, wild-type (WT) Akt, both WT Akt and CTMP, myr-Akt, and both myr-Akt and CTMP. The MOI was 10 for each virus. At 12 h after infection cells were irradiated with UV-B, and 8 h after irradiation MTT was added. MTT uptake was assayed by absorption at 570 nm. Some of the *t*-test results are shown in the table (*bottom*).

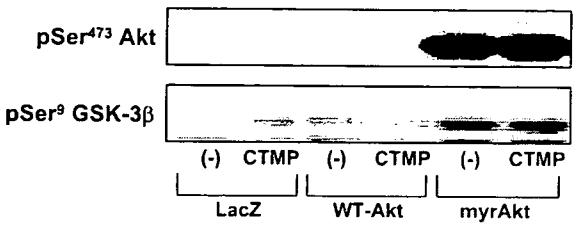

comparison		p value
LZ	CTMP	0.0002
LZ	WT-Akt	<0.0001
CTMP	WT-Akt + CTMP	<0.0001
WT-Akt	WT-Akt + CTMP	0.0002
myrAkt	myrAkt + CTMP	NS

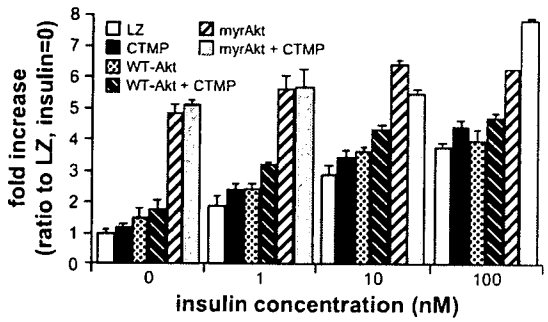

Fig. 7. 2-Deoxyglucose uptake assay in 3T3-L1 adipocytes. 3T3-L1 adipocytes were infected with adenovirus in 6 combinations, as described in Fig. 5, at an MOI of 100 for each virus. The phosphorylations of Akt and GSK-3β were investigated for each of these combinations and are shown at *top*. The blot is representative of 4 independent experiments, and the CTMP-induced increase in Akt phosphorylation was observed when WT-Akt was compared with WT-Akt + CTMP. A CTMP-induced increase in GSK-3β phosphorylation was observed in the comparison between LacZ and CTMP. No such significant differences were seen under the insulin-stimulated conditions (data not shown). 2-deoxy-D-[^{3}H]glucose uptakes with 0, 1, 10, and 100 nM insulin stimulation for 15 min were assayed twice each and are presented graphically at *bottom*. Repeated-measures 2-way ANOVA was conducted to detect the significance of differences in glucose uptake between pairs of viral conditions, and several of the results are shown in the table (*middle*).

compared with LacZ, but the difference was not significant. When Akt was coexpressed, CTMP showed a marked and significant antiapoptotic effect. myr-Akt, a well-known constitutively active type of Akt, also showed an apparent antiapoptotic effect.

CTMP expression in 3T3-L1 adipocytes modestly enhanced glucose uptake. Akt activation is known to induce glucose uptake of adipocytes via translocation of GLUT4 to the plasma membrane. We investigated the effect of CTMP overexpression on the glucose transport activity of 3T3-L1 adipocytes (Fig. 7). The CTMP overexpression level in 3T3-L1 adipocytes is much lower, even with the adenoviral transfer system, than in other cell lines such as COS-1 or HepG2. Thus slightly increased Akt phosphorylation was observed only in the WT Akt-overexpressing cells in the basal state. Similarly, slightly increased GSK-3β phosphorylation was observed only in LacZ cells under basal conditions. While myr-Akt induced a fivefold increase in glucose uptake in the absence of insulin stimulation (30), CTMP overexpression induced a relatively mild (1.2-fold over that of LacZ) but significant increase in uptake. Insulin

dose-dependently increased glucose uptake. Comparison of both CTMP and WT Akt overexpression with Akt overexpression alone, in response to stimulation with each of the indicated concentrations of insulin, showed the additional augmenting effect of CTMP on glucose uptake to be significant, although also of a modest degree (20% increase). This observation suggests that the effects of CTMP and Akt on glucose uptake are additive and more significant than that of the LacZ control.

CTMP expression in 3T3-L1 adipocytes enhanced glycogen synthesis. Since Akt is also known to enhance glycogenesis via inhibition of GSK-3β, the effect of CTMP on glycogenesis in 3T3-L1 adipocytes was investigated (Fig. 8). With insulin stimulation, glycogen synthesis increased in a dose-dependent manner in control LacZ-infected cells. Since the effect of CTMP plus Akt was observed to differ between low-dose and high-dose insulin conditions, statistical analyses were performed separately for the low- and high-dose groups. CTMP expression significantly enhanced glycogen synthesis. The magnitude of this enhancement was high when cells were stimulated with low concentrations of insulin (0.1 and 1 nM). However, the synergistic effect of CTMP and WT Akt overexpressions on glycogen synthesis was observed only in the nonstimulated state. On the other hand, constitutively active Akt (myr-Akt) markedly increased glycogen synthesis in the basal state. However, when stimulated with a high concentration of insulin (100 nM), myr-Akt expression suppressed glycogen synthesis. This finding suggests that when the Akt signaling pathway is highly stimulated for a long period, some negative feedback suppression(s) is exerted on the glycogen synthetic pathway (insulin desensitization). Comparing 3T3-L1 adipocytes expressing solely WT Akt and those coexpressing WT Akt and CTMP, glycogen synthesis was higher in the latter when the cells were unstimulated or stimulated with a low concentration of insulin (0 or 0.1 nM). In contrast, glycogen synthesis was higher in the former when cells were stimulated with higher concentrations of insulin (1 and 100 nM). This is attributable to the same desensitization mechanism.

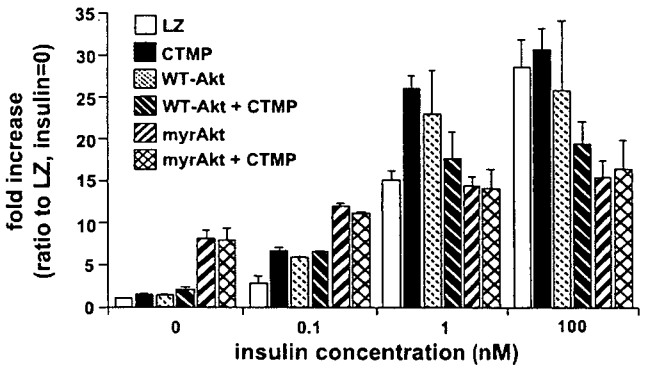

comparison		p value
LZ	CTMP	0.0001
LZ	WT-Akt	0.0027
CTMP	WT-Akt + CTMP [ins=0, 0.1]	NS
CTMP	WT-Akt + CTMP [ins=1, 100]	0.0003
WT-Akt	WT-Akt + CTMP [ins=0, 0.1]	0.0395
WT-Akt	WT-Akt + CTMP [ins=1, 100]	0.0123
myrAkt	myrAkt + CTMP	NS

Fig. 8. Glycogen assay in 3T3-L1 adipocytes. 3T3-L1 adipocytes were infected with adenovirus in 6 combinations, as described in Fig. 5, at an MOI of 100 for each virus. [U-^{14}C]glucose incorporations into glycogen with 3 h of 0, 0.1, 1, or 100 nM insulin stimulation were each assayed twice. Repeated-measured 2-way ANOVA was conducted to detect the significance of differences between pairs of viral conditions, and several of the results are shown in the table. The comparison between CTMP and WT-Akt + CTMP, and that between WT-Akt and WT-Akt + CTMP, showed the effects of interactions. Therefore, data obtained with the lower (0, 0.1 nM) and higher (1, 100 nM) doses of insulin were analyzed separately for these 2 cases.

DISCUSSION

Akt is activated by 3-phosphoinositides and PDKs, but there exist several proteins that bind to Akt and modulate its activation state (2, 4, 14, 34, 40). CTMP was reportedly shown to bind to the carboxy terminus of Akt and to inhibit its phosphorylation and activation. However, our repeated careful experiments demonstrated that CTMP enhanced the phosphorylation and activation of Akt and its downstream signal pathways, regardless of whether a transient or a stable expression system was used. Furthermore, siRNA-mediated suppression of CTMP inhibited Akt phosphorylation. However, this suppression was minimal, possibly suggesting that the presence of a substantial basal level of Akt is required for CTMP to be functional in HeLa cells. These findings are quite contrary to those of a previous report (34), but this discrepancy is not attributable to differences in the cell line or the method used for transfection, because we utilized various cell lines and obtained essentially the same results. Thus we cannot explain the different conclusions.

CTMP is reportedly located mainly on the plasma membrane. Indeed, we found that overexpression of CTMP markedly enhances membrane localization of Akt. From this finding, we speculate that the mechanism underlying the enhancing effect of CTMP on Akt phosphorylation involves translocation of Akt to the plasma membrane. It is well established that, with targeting to the membrane, Akt conformational change occurs such that Thr^{308} and Ser^{473} are presented to the outside of the Akt molecule and phosphorylated by PDKs (36).

In the aforementioned previous report, the authors suggested that CTMP on the plasma membrane binds to Akt in the basal state and that CTMP binding to Akt does not completely block Akt phosphorylation in the stimulated state, but rather makes it more difficult. After phosphorylation is achieved, Akt would presumably disassociate from CTMP. However, this theory is somewhat difficult to understand, because it is unclear how CTMP suppresses Akt activation in the stimulated state, despite dissociating from Akt in that state.

Our interpretations appear to be more reasonable and are easier to understand: Akt is located mainly in the cytosol in the basal state, and CTMP, which is always on the plasma membrane, recruits Akt from the cytosol to the plasma membrane, leading to the phosphorylation of Thr^{308} and Ser^{473} of Akt by PDKs. Indeed, CTMP-induced membrane translocation of Akt was observed in the presence of wortmannin. We also confirmed that CTMP does not influence PI3-kinase activity, suggesting that the effects of CTMP on Akt are direct. However, the PI3-kinase inhibitor LY-294002 dephosphorylates CTMP-induced Akt phosphorylation. This finding indicates that CTMP-induced Akt phosphorylation is maintained by basal PI3-kinase activity and/or basal concentrations of 3-phos-

phoinositides. In addition, as shown in Fig. 5, the total amount of Akt may be slightly increased. We speculate that CTMP induces translocation of Akt to the membrane, and that membrane-bound Akt thereby becomes susceptible to phosphorylation by upstream kinases such as PDK-1, which requires PI3-kinase activation, and phosphorylation of Thr^{308} and Ser^{473} by PDKs. It is also likely that CTMP increases the stability of Akt, possibly because of the increased amount of Akt.

To evaluate whether CTMP influences the antiapoptotic function of Akt, we combined UV-B irradiation (20) and MTT assay (15) in HeLa cells. The result showed clearly that CTMP enhances antiapoptosis, especially with Akt coexpression. In the previous report, the authors showed stable expression of CTMP in AKT8 tumor cells to inhibit tumor growth. Their experiment was designed to observe tumor growth, which is a more integrated cellular process than a specific antiapoptotic function. Moreover, AKT8 cells highly express constitutively active Akt, and the apoptotic signal in these cells may differ from that in physiological cells. On the other hand, our experiment induced relatively short-term CTMP expression in HeLa cells, in which Akt signaling would be nearer to physiological conditions. Therefore, we believe that our results reflect the physiological function of CTMP, at least as regards the antiapoptotic effect.

Akt reportedly plays critical roles in insulin-induced glucose metabolism, i.e., glycogen synthesis and glucose uptake. As for glycogen synthesis, Akt has been established as directly phosphorylating and inactivating GSK-3β, which results in activation of glycogen synthase. As for glucose uptake, constitutively active Akt reportedly induces GLUT4 translocation, thereby increasing glucose uptake. Our experiments revealed that CTMP enhances both of these pathways, indicating that CTMP may function as an insulin-sensitizing molecule for glucose metabolism, possibly in relation to insulin sensitivity. In the glycogen synthesis assay, expression of myr-Akt, or coexpression of CTMP and Akt, induced insulin desensitization. This phenomenon may be attributable to glycogen synthesis not being regulated solely by the insulin/Akt/GSK-3β/glycogen synthase pathway but also by the insulin/protein phosphatase-1 pathway (10, 42), which may be suppressed by chronic Akt activation. At a minimum, the desensitization occurred in response to both myr-Akt expression and Akt-CTMP coexpression, which is consistent with our finding that CTMP strongly activates coexpressed Akt. On the other hand, the effects of CTMP on insulin-induced glucose uptake were modest, although statistically significant. From this finding, we speculate that CTMP leads to Akt activation mainly on the plasma membrane, while for efficient GLUT4 translocation activation of Akt in other intracellular compartments may be critical.

Recently, we (2) and another group (17) have identified a novel 200-kDa protein that binds to the carboxy terminus of Akt and markedly enhances Akt phosphorylation. This protein was termed Akt phosphorylation enhancer (APE), or Girdin. We have the impression that APE/Girdin exerts more potent activity, markedly increasing Akt phosphorylation, although exact comparison is difficult. Taking into consideration that both APE/Girdin and CTMP bind to the carboxy terminus of Akt, the mechanisms underlying the increases in Akt phosphorylation may be similar. We speculate that their binding to the carboxy terminus of Akt would induce conformational changes in Akt, thereby possibly making Akt more easily accessible to PDK-1 and PDK-2. Interestingly, APE/Girdin binds to actin, and CTMP is located at the plasma membrane. Thus both APE/Girdin and CTMP enhance Akt activity by modifying the conformation of the Akt carboxy terminus, but the former may function by interacting with the actin network and the latter at the plasma membrane. Further work is necessary to elucidate the similarities and differences in these proteins.

In summary, our experimental findings on CTMP overexpression and suppression in various cell systems allow us to draw the conclusion that CTMP enhances Akt phosphorylation and activation. The mechanism appears to involve membrane-localized CTMP recruiting Akt from the cytosol to the plasma membrane. CTMP-induced Akt activation results in phosphorylation of Akt substrates. It also activates multiple downstream Akt pathways, including antiapoptotic, glycogen synthetic, and glucose uptake processes. Therefore, CTMP may be involved in cellular antiapoptotic mechanisms and insulin sensitivity.

REFERENCES

1. **Alessi DR, Cohen P.** Mechanism of activation and function of protein kinase B. *Curr Opin Genet Dev* 8: 55–62, 1998.
2. **Anai M, Shojima N, Katagiri H, Ogihara T, Sakoda H, Onishi Y, Ono H, Fujishiro M, Fukushima Y, Horike N, Viana A, Kikuchi M, Noguchi N, Takahashi S, Takata K, Oka Y, Uchijima Y, Kurihara H, Asano T.** A novel protein kinase B (PKB)/AKT-binding protein enhances PKB kinase activity and regulates DNA synthesis. *J Biol Chem* 280: 18525–18535, 2005.
3. **Asano T, Takata K, Katagiri H, Tsukuda K, Lin JL, Ishihara H, Inukai K, Hirano H, Yazaki Y, Oka Y.** Domains responsible for the differential targeting of glucose transporter isoforms. *J Biol Chem* 267: 19636–19641, 1992.
4. **Brazil DP, Park J, Hemmings BA.** PKB binding proteins. Getting in on the Akt. *Cell* 111: 293–303, 2002.
5. **Brunet A, Bonni A, Zigmond MJ, Lin MZ, Juo P, Hu LS, Anderson MJ, Arden KC, Blenis J, Greenberg ME.** Akt promotes cell survival by phosphorylating and inhibiting a Forkhead transcription factor. *Cell* 96: 857–868, 1999.
6. **Burgering BM, Coffer PJ.** Protein kinase B (c-Akt) in phosphatidylinositol-3-OH kinase signal transduction. *Nature* 376: 599–602, 1995.
7. **Chan TO, Rittenhouse SE, Tsichlis PN.** AKT/PKB and other D3 phosphoinositide-regulated kinases: kinase activation by phosphoinositide-dependent phosphorylation. *Annu Rev Biochem* 68: 965–1014, 1999.
8. **Cheatham B, Vlahos CJ, Cheatham L, Wang L, Blenis J, Kahn CR.** Phosphatidylinositol 3-kinase activation is required for insulin stimulation of pp70 S6 kinase, DNA synthesis, and glucose transporter translocation. *Mol Cell Biol* 14: 4902–4911, 1994.
9. **Coffer PJ, Jin J, Woodgett JR.** Protein kinase B (c-Akt): a multifunctional mediator of phosphatidylinositol 3-kinase activation. *Biochem J* 335: 1–13, 1998.
10. **Cohen P.** The structure and regulation of protein phosphatases. *Annu Rev Biochem* 58: 453–508, 1989.
11. **Cross DA, Alessi DR, Cohen P, Andjelkovich M, Hemmings BA.** Inhibition of glycogen synthase kinase-3 by insulin mediated by protein kinase B. *Nature* 378: 785–789, 1995.
12. **Datta SR, Dudek H, Tao X, Masters S, Fu H, Gotoh Y, Greenberg ME.** Akt phosphorylation of BAD couples survival signals to the cell-intrinsic death machinery. *Cell* 91: 231–241, 1997.
13. **Downward J.** Mechanisms and consequences of activation of protein kinase B/Akt. *Curr Opin Cell Biol* 10: 262–267, 1998.
14. **Du K, Herzig S, Kulkarni RN, Montminy M.** TRB3: a tribbles homolog that inhibits Akt/PKB activation by insulin in liver. *Science* 300: 1574–1577, 2003.
15. **Eble MJ, Hensley FW, Flentje M, Schlotz A, Wannenmacher M.** A modified computer-assisted colorimetric microtitre assay (MTT) to assess in vitro radiosensitivity of V79, CaSki, HeLa and WiDr cells. *Int J Radiat Biol* 65: 193–201, 1994.

16. **Elstrom RL, Bauer DE, Buzzai M, Karnauskas R, Harris MH, Plas DR, Zhuang H, Cinalli RM, Alavi A, Rudin CM, Thompson CB.** Akt stimulates aerobic glycolysis in cancer cells. *Cancer Res* 64: 3892–3899, 2004.
17. **Enomoto A, Murakami H, Asai N, Morone N, Watanabe T, Kawai K, Murakumo Y, Usukura J, Kaibuchi K, Takahashi M.** Akt/PKB regulates actin organization and cell motility via Girdin/APE. *Dev Cell* 9: 389–402, 2005.
18. **Feng J, Park J, Cron P, Hess D, Hemmings BA.** Identification of a PKB/Akt hydrophobic motif Ser-473 kinase as DNA-dependent protein kinase. *J Biol Chem* 279: 41189–41196, 2004.
19. **Franke TF, Kaplan DR, Cantley LC, Toker A.** Direct regulation of the Akt proto-oncogene product by phosphatidylinositol-3,4-bisphosphate. *Science* 275: 665–668, 1997.
20. **French LE, Wohlwend A, Sappino AP, Tschopp J, Schifferli JA.** Human clusterin gene expression is confined to surviving cells during in vitro programmed cell death. *J Clin Invest* 93: 877–884, 1994.
21. **Hajduch E, Litherland GJ, Hundal HS.** Protein kinase B (PKB/Akt)—a key regulator of glucose transport? *FEBS Lett* 492: 199–203, 2001.
22. **Hanada M, Feng J, Hemmings BA.** Structure, regulation and function of PKB/AKT—a major therapeutic target. *Biochim Biophys Acta* 1697: 3–16, 2004.
23. **Hill MM, Hemmings BA.** Inhibition of protein kinase B/Akt. Implications for cancer therapy. *Pharmacol Ther* 93: 243–251, 2002.
24. **Hresko RC, Mueckler M.** mTOR·RICTOR is the Ser^{473} kinase for Akt/protein kinase B in 3T3-L1 adipocytes. *J Biol Chem* 280: 40406–40416, 2005.
25. **Iynedjian PB, Roth RA, Fleischmann M, Gjinovci A.** Activation of protein kinase B/cAkt in hepatocytes is sufficient for the induction of expression of the gene encoding glucokinase. *Biochem J* 351: 621–627, 2000.
26. **Kandel ES, Hay N.** The regulation and activities of the multifunctional serine/threonine kinase Akt/PKB. *Exp Cell Res* 253: 210–229, 1999.
27. **Katagiri H, Asano T, Ishihara H, Inukai K, Shibasaki Y, Kikuchi M, Yazaki Y, Oka Y.** Overexpression of catalytic subunit p110α of phosphatidylinositol 3-kinase increases glucose transport activity with translocation of glucose transporters in 3T3-L1 adipocytes. *J Biol Chem* 271: 16987–16990, 1996.
28. **Kawakami Y, Nishimoto H, Kitaura J, Maeda-Yamamoto M, Kato RM, Littman DR, Leitges M, Rawlings DJ, Kawakami T.** Protein kinase C βII regulates Akt phosphorylation on Ser-473 in a cell type- and stimulus-specific fashion. *J Biol Chem* 279: 47720–47725, 2004.
29. **Kennedy SG, Wagner AJ, Conzen SD, Jordan J, Bellacosa A, Tsichlis PN, Hay N.** The PI3-kinase/Akt signaling pathway delivers an anti-apoptotic signal. *Genes Dev* 11: 701–713, 1997.
30. **Kohn AD, Summers SA, Birnbaum MJ, Roth RA.** Expression of a constitutively active Akt Ser/Thr kinase in 3T3-L1 adipocytes stimulates glucose uptake and glucose transporter 4 translocation. *J Biol Chem* 271: 31372–31378, 1996.
31. **Kops GJ, Burgering BM.** Forkhead transcription factors: new insights into protein kinase B (c-akt) signaling. *J Mol Med* 77: 656–665, 1999.
32. **Liao J, Barthel A, Nakatani K, Roth RA.** Activation of protein kinase B/Akt is sufficient to repress the glucocorticoid and cAMP induction of phosphoenolpyruvate carboxykinase gene. *J Biol Chem* 273: 27320–27324, 1998.
33. **Lieber A, He CY, Kirillova I, Kay MA.** Recombinant adenoviruses with large deletions generated by Cre-mediated excision exhibit different biological properties compared with first-generation vectors in vitro and in vivo. *J Virol* 70: 8944–8960, 1996.
34. **Maira SM, Galetic I, Brazil DP, Kaech S, Ingley E, Thelen M, Hemmings BA.** Carboxyl-terminal modulator protein (CTMP), a negative regulator of PKB/Akt and v-Akt at the plasma membrane. *Science* 294: 374–380, 2001.
35. **Marte BM, Downward J.** PKB/Akt: connecting phosphoinositide 3-kinase to cell survival and beyond. *Trends Biochem Sci* 22: 355–358, 1997.
36. **Milburn CC, Deak M, Kelly SM, Price NC, Alessi DR, Van Aalten DM.** Binding of phosphatidylinositol 3,4,5-trisphosphate to the pleckstrin homology domain of protein kinase B induces a conformational change. *Biochem J* 375: 531–538, 2003.
37. **Ono H, Shimano H, Katagiri H, Yahagi N, Sakoda H, Onishi Y, Anai M, Ogihara T, Fujishiro M, Viana AY, Fukushima Y, Abe M, Shojima N, Kikuchi M, Yamada N, Oka Y, Asano T.** Hepatic Akt activation induces marked hypoglycemia, hepatomegaly, and hypertriglyceridemia with sterol regulatory element binding protein involvement. *Diabetes* 52: 2905–2913, 2003.
38. **Partovian C, Simons M.** Regulation of protein kinase B/Akt activity and Ser473 phosphorylation by protein kinase Cα in endothelial cells. *Cell Signal* 16: 951–957, 2004.
39. **Persad S, Attwell S, Gray V, Mawji N, Deng JT, Leung D, Yan J, Sanghera J, Walsh MP, Dedhar S.** Regulation of protein kinase B/Akt-serine 473 phosphorylation by integrin-linked kinase: critical roles for kinase activity and amino acids arginine 211 and serine 343. *J Biol Chem* 276: 27462–27469, 2001.
40. **Remy I, Michnick SW.** Regulation of apoptosis by the Ft1 protein, a new modulator of protein kinase B/Akt. *Mol Cell Biol* 24: 1493–1504, 2004.
41. **Sakoda H, Gotoh Y, Katagiri H, Kurokawa M, Ono H, Onishi Y, Anai M, Ogihara T, Fujishiro M, Fukushima Y, Abe M, Shojima N, Kikuchi M, Oka Y, Hirai H, Asano T.** Differing roles of Akt and serum- and glucocorticoid-regulated kinase in glucose metabolism, DNA synthesis, and oncogenic activity. *J Biol Chem* 278: 25802–25807, 2003.
42. **Saltiel AR.** Diverse signaling pathways in the cellular actions of insulin. *Am J Physiol Endocrinol Metab* 270: E375–E385, 1996.
43. **Sarbassov DD, Guertin DA, Ali SM, Sabatini DM.** Phosphorylation and regulation of Akt/PKB by the rictor-mTOR complex. *Science* 307: 1098–1101, 2005.
44. **Sen P, Mukherjee S, Ray D, Raha S.** Involvement of the Akt/PKB signaling pathway with disease processes. *Mol Cell Biochem* 253: 241–246, 2003.
45. **Stephens L, Anderson K, Stokoe D, Erdjument-Bromage H, Painter GF, Holmes AB, Gaffney PR, Reese CB, McCormick F, Tempst P, Coadwell J, Hawkins PT.** Protein kinase B kinases that mediate phosphatidylinositol 3,4,5-trisphosphate-dependent activation of protein kinase B. *Science* 279: 710–714, 1998.
46. **Stokoe D, Stephens LR, Copeland T, Gaffney PR, Reese CB, Painter GF, Holmes AB, McCormick F, Hawkins PT.** Dual role of phosphatidylinositol-3,4,5-trisphosphate in the activation of protein kinase B. *Science* 277: 567–570, 1997.
47. **Summers SA, Birnbaum MJ.** A role for the serine/threonine kinase, Akt, in insulin-stimulated glucose uptake. *Biochem Soc Trans* 25: 981–988, 1997.
48. **Ueki K, Yamamoto-Honda R, Kaburagi Y, Yamauchi T, Tobe K, Burgering BM, Coffer PJ, Komuro I, Akanuma Y, Yazaki Y, Kadowaki T.** Potential role of protein kinase B in insulin-induced glucose transport, glycogen synthesis, and protein synthesis. *J Biol Chem* 273: 5315–5322, 1998.
49. **van Weeren PC, de Bruyn KM, de Vries-Smits AM, van Lint J, Burgering BM.** Essential role for protein kinase B (PKB) in insulin-induced glycogen synthase kinase 3 inactivation. Characterization of dominant-negative mutant of PKB. *J Biol Chem* 273: 13150–13156, 1998.
50. **Weigert C, Hennige AM, Brodbeck K, Haring HU, Schleicher ED.** Interleukin-6 acts as insulin sensitizer on glycogen synthesis in human skeletal muscle cells by phosphorylation of Ser^{473} of Akt. *Am J Physiol Endocrinol Metab* 289: E251–E257, 2005.
51. **Whiteman EL, Cho H, Birnbaum MJ.** Role of Akt/protein kinase B in metabolism. *Trends Endocrinol Metab* 13: 444–451, 2002.
52. **Yamada T, Katagiri H, Asano T, Inukai K, Tsuru M, Kodama T, Kikuchi M, Oka Y.** 3-Phosphoinositide-dependent protein kinase 1, an Akt1 kinase, is involved in dephosphorylation of Thr-308 of Akt1 in Chinese hamster ovary cells. *J Biol Chem* 276: 5339–5345, 2001.

0013-7227/07/$15.00/0
Printed in U.S.A.

Endocrinology 148(10):4658–4666

doi: 10.1210/en.2007-0296

Social Isolation Affects the Development of Obesity and Type 2 Diabetes in Mice

Katsunori Nonogaki, Kana Nozue, and Yoshitomo Oka

Center of Excellence, Division of Molecular Metabolism and Diabetes, Tohoku University Graduate School of Medicine, Miyagi 980-8575, Japan

Social isolation is associated with increased risks of mortality and morbidity. In this study, we show that chronic individual housing accelerated body weight gain and adiposity in KK mice but not C57BL6J mice, and fully developed diabetes in KKA^y mice. Individually housed KK and KKA^y mice increased body weight gain over the initial 2 wk without increased daily average food consumption compared with group-housed animals. The individually housed KK and KKA^y mice then gradually increased food consumption for the next 1 wk. The chronic social isolation-induced obesity (SIO) was associated with hyperleptinemia and lower plasma corticosterone and active ghrelin levels but not hyperinsulinemia. Elevated plasma leptin in the SIO suppressed expression of 5-HT2C receptor in white adipose tissue. The SIO was also associated with decreased expression of β3-adrenergic receptors in white adipose tissue and hypothalamic leptin receptor, which might be secondary to the enhanced adiposity. Interestingly, social isolation acutely reduced food consumption and body weight gain compared with group-housed obese db/db mice with leptin receptor deficiency. Social isolation-induced hyperglycemia in KKA^y mice was associated with increased expression of hepatic gluconeogenetic genes independent of insulin. These findings suggest that social isolation promotes obesity due to primary decreased energy expenditure and secondary increased food consumption, which are independent of the disturbed leptin signaling, in KK mice, and develops into insulin-independent diabetes associated with increased expression of hepatic gluconeogenetic genes in KKA^y mice. Thus, social isolation can be included in the environmental factors that contribute to the development of obesity and type 2 diabetes. (*Endocrinology* 148: 4658–4666, 2007)

SOCIAL ISOLATION OR lack of social support is associated with increased risks for mortality (1, 2) and negative health outcomes, including heart disease, hypertension, stroke, and arthritis (3–7). Excess body weight during midlife is also associated with an increased risk factor of mortality and the negative health outcomes (8). However, interesting aspects of the relationship between social isolation and development of obesity remain to be resolved. Although individually housed Swiss CD-1 mice and Wistar rats do not grow as fast as group-housed ones (9–11), animal models of social isolation-induced obesity (SIO) and type 2 diabetes have yet to be identified.

The KK mice have long been included in the group of animals that become obese and develop diabetes, as have the A^y mice. The A^y yellow mice are known to become obese, and when bred with the KK mice, the development of diabetes is more pronounced. To determine the effects of social isolation on the development of obesity and type 2 diabetes, we examined the effects of individual and group housing on body weight, adipose tissues, plasma hormone levels, and expression of genes involved in the regulation of energy homeostasis in C57BL6J, KK, and KKA^y mice.

First Published Online July 19, 2007

Abbreviations: β3-AR, β3-Adrenergic receptor; BAT, brown adipose tissue; CNS, central nervous system; Fbp, fructose bisphosphatase; G6Pase, glucose-6-phosphatase; MC, melanocortin; PEPCK, pyruvate carboxykinase; SIO, social isolation-induced obesity; SOCS-3, suppressor of cytokine signaling 3; UCP, uncoupling protein.

***Endocrinology* is published monthly by The Endocrine Society (http://www.endo-society.org), the foremost professional society serving the endocrine community.**

Materials and Methods

General procedures

Four-week-old male C57BL6J mice, KK, and KKA^y mice and 8-wk-old db/db mice were purchased from Japan CLEA (Tokyo, Japan). After the arrival of the animals, all mice were group-housed and acclimated to the colony for 1 wk before the experiment. Before the experiment, they were all housed (three to four mice per cage) with free access to water and chow pellets in a light (12 h on/12 h off; lights off at 2000 h)- and temperature (20–22 C)-controlled environment. One week later, animals were randomly transferred to individually housed conditions. Mice were housed in groups of three to four per cage (21.5 × 32 × 14 cm) or individually for 3 wk preceding decapitation. Their body weights were measured every 7 d in the morning for 3 wk. The average amounts of daily food consumption per week were evaluated in 5- to 8-wk-old animals.

Administration of drugs

Four-week-old C57BL6J mice were individually housed in standard mouse cages with free access to food and water for 1 wk before testing. Mice were injected ip with saline or leptin (5 mg/kg). They were not fed chow pellets. Sixty minutes later, the animals were decapitated and the epididymal white adipose tissue was removed for RNA extraction. The experiment was performed between 1000–1200 h. The dose of leptin (5 mg/kg) was selected based on the evidence that leptin induced hypophagia and decreases in body weights in 5-HT2C receptor mutant and wild-type mice (12).

Blood chemistries

Plasma ghrelin and adiponectin levels were measured by ELISA using an active ghrelin ELISA kit and des-acyl ghrelin ELISA kit (Mitsubishi Kagaku Iatron Inc., Tokyo, Japan) and mouse adiponectin ELISA kit (Ootsuka Inc., Tokyo, Japan). For the ELISA of active ghrelin, 1 N hydrogen chloride was added to the samples at a final concentration of 0.1 N immediately after plasma separation. Plasma leptin, insulin, and corticosterone levels were measured using mouse leptin (Linco, St. Louis, MO), rat insulin (Linco), and rat corticosterone (ICN Biomedicals,

Costa Mesa, CA) RIA kits, respectively. Blood glucose levels were measured using glucose strips (blood glucose monitoring system; FreeStyle; KISSEI, Tokyo, Japan).

The animal studies were conducted under protocols in accordance with the institutional guidelines for animal experiments at Tohoku University Graduate School of Medicine.

Real-time quantitative RT-PCR

Total RNA was extracted from the epididymal white adipose tissue, brown adipose tissue (BAT), and soleus skeletal muscle by the acid-isolated guanidium thiocyanate-phenol-chloroform method and was isolated from mouse liver and hypothalamic tissue using the RNeasy Midi kit (Qiagen, Hilden, Germany) according to the manufacturer's directions. cDNA synthesis was performed using a Super Script III First-Strand Synthesis System for RT-PCR Kit (Invitrogen, Rockville, MD) using 1 μg total RNA. cDNA synthesized from total RNA was evaluated in a real-time PCR quantitative system (Light Cycler Quick System 350S; Roche Diagnostics, Mannheim, Germany). The primers used are listed in Table 1.

The relative amount of mRNA was calculated using β-actin mRNA as the invariant control. The data are shown as the fold change of the mean value of the control group, which received saline.

Data are presented as the mean values ± SEM (n = 5–8). Comparisons between the two groups were performed using two-tailed unpaired Student's *t* test. Comparisons among more than two groups were done by ANOVA using Bonferroni's test. The presence of a linear correlation was assessed using a parametric (Pearson's) correlation test. A *P* value of less than 0.05 was considered statistically significant.

TABLE 1. The primers used for real-time RT-PCR

Gene	Primer	Sequence
LepR	Sense	CTGAATTTCCAAAAGCCTGA
	Antisense	AAGCTGTATCGACACTGATTTC
MC4R	Sense	GAGGTGTTTGTGACTCTGGG
	Antisense	GAACATGTGGACATAGAGAG
5-HT2CR	Sense	CTGAGGGACGAAAGCAAAG
	Antisense	CACATAGCCAATCCAAACAAAC
5-HT1BR	Sense	TGCCTGCTGGTTTCACAT
	Antisense	GCGCACTTAAAGCGTATCA
SOCS-3	Sense	GCGGGCACCTTTCTTATCC
	Antisense	TCCCCGACTGGGTCTTGAC
β3-AR	Sense	ATGGCTCCGTGGCCTCAC
	Antisense	CCCAACGGCCAGTGGCCAGTCAGCG
UCP-1	Sense	GACAGTACCCAAGCGTACCAA
	Antisense	CATGATGACGTTCCAGGACC
UCP-2	Sense	GTTCCTCTGTCTCGTCTTGC
	Antisense	GGCCTTGAAACCAACCA
UCP-3	Sense	GTTGCTGGAGTCTCACCTGT
	Antisense	TCTTCAGCATACAGTGCAGA
PPARα	Sense	CGGGTAACCTCGAAGTCTGA
	Antisense	CTAACCTTGGGCCACACCT
PPARγ	Sense	CTGCTCAAGTATGGTGTCCATGAG
	Antisense	GAGGAACTCCCTGGTCATGAATC
PPARδ	Sense	GCTGCTGCAGAAGATGGCA
	Antisense	CACTGCATCATCTGGGCATG
G6Pase	Sense	TGCAAGGGAGAACTCAGCAA
	Antisense	GGACCAAGGAAGCCACAATG
Fbp1	Sense	TCTGCACCGCGATCAAAG
	Antisense	GTTGAGCCAGCGATACCATAGAG
Fbp2	Sense	AGAAAGACCACGGAGGACGA
	Antisense	CCCGCAGCCACGATGT
PEPCK	Sense	AGCGGATATGGTGGGAAC
	Antisense	GGTCTCCACTCCTTGTTC
β-actin	Sense	TTGTAACCAACTGGGACGATATGG
	Antisense	GATCTTGATCTTCATGGTGCTAGG

Results

Changes in body weight and adipose tissue weight in individually and group-housed C57BL6J mice and KK mice

There were no significant differences in body weight change between individually housed and group-housed C57BL6J mice for 3 wk in 6- to 8-wk-old animals (Fig. 1A), whereas the increases in body weight were significantly greater in individually housed KK mice than those in group-housed ones after 6 wk of age (Fig. 1B). Epididymal white adipose tissue and BAT weight significantly increased in 8-wk-old individually housed KK mice compared with group-housed ones, whereas there were no differences between individually housed and group-housed C57BL6J mice (Fig. 1, C and D). These findings indicate that chronic social isolation accelerates body weight gain and adiposity in KK mice but not C57BL6J mice.

Plasma chemistries in individually housed and group-housed KK mice

To determine the characteristics of obesity induced by chronic social isolation, we examined blood chemistries in individually housed and group-housed 8-wk-old C57BL6J and KK mice. Plasma leptin levels were significantly elevated in individually housed 8-wk-old KK mice compared with group-housed ones (15.5 ± 1.1 *vs.* 6.01 ± 0.55 ng/ml, $P < 0.05$). There were no significant differences in plasma insulin levels between the individually housed and group-housed 8-wk-old KK mice (5.34 ± 0.94 *vs.* 3.90 ± 0.62 ng/ml). Plasma corticosterone and active ghrelin, but not des-acyl ghrelin, levels were significantly decreased in the individually housed 8-wk-old KK mice compared with group-housed ones (corticosterone, 23.9 ± 2.7 *vs.* 56.3 ± 11.9 ng/ml, $P < 0.05$; active ghrelin, 8.72 ± 0.94 *vs.* 14.88 ± 1.37 fmol/ml, $P < 0.05$; and des-acyl ghrelin, 258 ± 21.0 *vs.* 288 ± 30.17 fmol/ml). There were no significant differences in the plasma adiponectin or blood glucose levels between the individually housed and group-housed 8-wk-old KK mice (adiponectin, 7.12 ± 0.29 *vs.* 7.62 ± 0.59 μg/ml; glucose, 156 ± 9 *vs.* 160 ± 5 mg/dl). These hormonal and metabolic alterations induced by social isolation in KK mice were not found in C57BL6J mice (data not shown). These findings suggest that chronic SIO is not due to hyperinsulinemia or hypercorticosteronemia, and is not associated with decreases in plasma adiponectin or des-acyl ghrelin levels.

Altered expression of genes involved in energy homeostasis and daily food consumption of individually housed and group-housed KK mice

To further determine the characteristics of chronic SIO associated with hyperleptinemia in the individually housed and group-housed 8-wk-old KK mice (Fig. 2A), we examined the expression of hypothalamic leptin receptor (Ob-Rb; *LepR*), melanocortin (MC)-4 receptor, and 5-HT2C receptor, which are involved in the central regulation of feeding behavior and energy homeostasis (13). Hypothalamic *LepR* mRNA levels were significantly decreased in the individually housed 8-wk-old KK mice compared with group-housed mice (24% decrease), although there were no significant dif-